




periodic table of the "lighting" elements

H																	He
Li	Be											B	C	N	O	F	Ne
Na	Mg											Al	Si	P	S	Cl	Ar
K	Ca	Sc	Ti	V	Cr	Mn	Fe	Co	Ni	Cu	Zn	Ga	Ge	As	Se	Br	Kr
Rb	Sr	Y	Zr	Nb	Mo	Tc	Ru	Rh	Pd	Ag	Cd	In	Sn	Sb	Te	I	Xe
Cs	Ba	La	Hf	Ta	W	Re	Os	Ir	Pt	Au	Hg	Tl	Pb	Bi	Po	At	Rn
Fr	Ra	Ac															
			Ce	Pr	Nd	Pm	Sm	Eu	Gd	Tb	Dy	Ho	Er	Tm	Yb	Lu	
			Th	Pa	U	Np	Pu	Am	Cm	Bk	Cf	Es	Fm	Md	No	Lr	

-  activator elements
-  plasma elements
-  host lattice elements

New Developments in the Field of Luminescent Materials for Lighting and Displays

Thomas Jüstel,* Hans Nikol,* and Cees Ronda*

While in the seventies and eighties the field of luminescent materials seemed to be fairly well covered, research in the nineties has been revitalized both in industry and academia. Improved performance of allegedly mature “classical” materials has demonstrated impressively the role of until then often neglected parameters such as surface and particle properties. In a business as developed as the lamp market new lamp features such as reduced mercury consumption can lead to a competitive edge and new phosphor research pro-

grams. Quantum cutter phosphors that generate two visible photons from one UV photon are the focus of research again, for example, for plasma display panels as huge flat and thin hang-on-the-wall TVs. Promising new developments such as electroluminescent full-color displays or the blue (laser) diode have created excitement and numerous research efforts in laboratories around the world. The direct conversion of electricity into light, common to both applications, challenges current concepts and might eventually revolu-

tionize the way we illuminate rooms, car lights, or traffic signals, and how we display video information. A deep understanding of the interaction of light and matter together with advanced material chemistry is the key to both improved and new lighting and display products.

Keywords: displays • fluorescence • luminescence • materials science • rare-earth compounds

1. Introduction

Luminescent materials, also called phosphors, can be found in a broad range of every-day applications such as cathode ray tubes (CRTs^[**]), projection televisions (PTVs), fluorescent tubes, and X-ray detectors, to name just the most important.^[1, 2] Improvements over the last three decades have led to phosphor materials that operate close to their physical limits. It cannot be expected that properties such as quantum yield and spectral energy distribution will be significantly improved or that distinctly better materials will be found in the near future.

Although the phosphor selection for CRTs and fluorescent lamps was made long ago there is still considerable research activity to improve the chemical stability and to adapt the materials to the production technology of the respective application.^[3, 4] Ongoing miniaturization, lifetime improvement, and spectral stability of fluorescent lamps on the one hand and brightness and contrast improvement in imaging systems on the other hand demand luminescent materials with very high stability that is invariable to operating conditions.

The conditioning of the surface of the phosphor grains is a major research target these days to obtain luminescent materials with improved performance. This conditioning is achieved mainly by a chemical refining step after the synthesis or by an additional coating on the particle surface.^[5, 6] Ideally, the chemical behavior is altered in such a way that a suspension of the phosphor material in water or an organic medium becomes more stable during the manufacturing process as well as under the harsh operating conditions in discharge lamps or TV tubes (i.e. electron and ion bombardment, respectively, as well as plasma interaction). Contrary to classical areas of application the search for new materials is most important for tomorrow's fields of light generation for displays and illumination. The research area is best organized by the excitation source. Luminescent materials in plasma display panels (PDP) and field emission displays (FED) use the high-energy side of the UV spectrum, that is vacuum ultraviolet (VUV) and even low voltage electrons, respectively. Phosphors on light emitting diodes (LED) and to some extent in fluorescent lamps for special applications are excited by near UV or blue light. Probably the most revolutionary is the direct excitation of semiconductors by electrical current in LEDs and of both organic and inorganic phosphor materials by organic and inorganic electroluminescence (EL), respectively. Consequently, the search for new materials is performed vigorously in industry and university laboratories. Thereby, classical doped solid-state materials are increasingly

[*] Dr. T. Jüstel, H. Nikol, C. Ronda
Philips Research Laboratories
Weissshausstrasse 2, D-52066 Aachen (Germany)
Fax: (+49) 241-6003-483
E-mail: juestel@pfa.research.philips.com

[**] A list of the abbreviations used can be found in the Appendix.

giving way to new material classes such as doped zeolites, organic phosphors, and composite and nanosized materials.

After a brief introduction of the physical background of luminescent materials, the current situation for lighting applications and display technology is described in separate sections. New technologies and their impact on the research of luminescent materials follow together with a discussion of upcoming trends in this field of material research.

2. Basic Aspects of Luminescent Materials

Light of appropriate spectral distribution in discharge lamps or imaging systems is nowadays mostly generated with luminescent materials that act as the final partner in the energy transfer chain and emit photons in the visible, UV or IR spectral range (Figure 1). The photon emission of a

material following energy supply is generally called luminescence. Several types of luminescence can be distinguished depending on the excitation source (Table 1).

Table 1. Different forms of luminescence.

Luminescence type	Excitation source	Application
cathodoluminescence	electrons	TV sets, monitors
photoluminescence	(UV) photons	fluorescent lamps, plasma displays
X-ray luminescence	X-rays	X-ray amplifier
electroluminescence	electric field	LEDs, EL displays
sonoluminescence	ultrasound	
solvatoluminescence	photons	detectors, analytical devices
chemoluminescence	chemical reaction energy	analytical chemistry
bioluminescence	biochemical reaction energy	analytical chemistry
triboluminescence	mechanical energy	

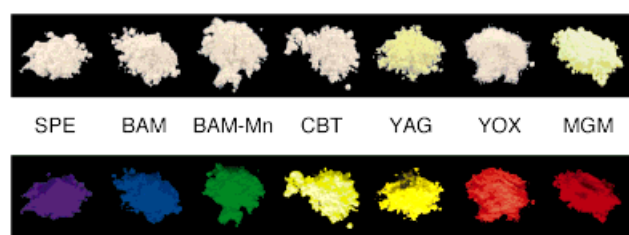


Figure 1. Commercial phosphor powders commonly applied in fluorescent lamps and displays. Top: under white light illumination; bottom: under irradiation with UV light (254 nm excitation wavelength). For an explanation of abbreviations and application areas: see Tables 2–4 and 6, and Section 3, respectively.

While sono-,^[7] solvato-, chemo-, bio-, and triboluminescence are currently not used in lighting and display applications, quite a variety of materials has been developed for all other forms of luminescence. They can be divided into inorganic and organic phosphors; the former being mainly solid-state compounds that consist of crystals 1–10 μm in size, while the latter can either be polymers or low molecular weight materials applied as thin films or solid solutions.

“Classical” inorganic phosphors usually consist of a host lattice with activator ions doped into it in small concentrations, typically a few mole percent or less. The activator ions possess energy levels that can be populated by direct

Thomas Jüstel was born in Witten in 1968. He studied chemistry at the University of Bochum from 1987 to 1992. He received his Ph. D. in coordination chemistry in 1995 in the group of Prof. Dr. K. Wieghardt. After spending half a year as a postdoctoral fellow at the MPI Mülheim für Strahlenchemie he entered the Philips Research Laboratory in Aachen in september 1995. He is currently working on luminescent materials for lamps and display applications.



T. Jüstel



H. Nikol



C. Ronda

Hans Nikol was born in 1966 and studied chemistry at the University of Regensburg from 1985 to 1990. He completed his Ph. D. in photochemistry in 1993 in the group of Prof. Dr. A. Vogler. The following two years he spent as a postdoctoral research fellow at the California Institute of Technology in the group of Prof. H. B. Gray. He joined the Philips Research Laboratory in Aachen in 1995 where he is working on luminescent materials for lamps and display applications.

Cees Ronda was born in Groningen, the Netherlands in 1959. He studied Solid State and Theoretical Chemistry at the State University of Groningen where he also obtained his doctorate degree. His thesis dealt with optical and electrical properties of layered metal chalcogenides and halides. In 1986 he joined Philips Research Laboratories in Eindhoven, the Netherlands. In 1989, he went to the Philips Research Laboratories in Aachen. Since joining Philips he has been studying luminescent materials for lamps and display applications.

excitation or indirectly by energy transfer, and are responsible for the luminescence. Generally, two types of activator ions can be distinguished. In the first type the energy levels of the activator ion involved in the emission process show only weak interactions with the host lattice. Typical examples are many of the lanthanide ions Ln^{3+} , where the optical transitions take place solely between 4f terms that are well shielded from their chemical environment by outer electrons. As a consequence characteristic line emission spectra can be observed.

The second type of activator ions strongly interact with the host lattice. This is the case when d electrons are involved, for example, in Mn^{2+} , Eu^{2+} , and Ce^{3+} , as well as for s^2 ions like Pb^{2+} or Sb^{3+} , or for complex anions such as MoO_4^{2-} or NbO_3^{3-} . The strong coupling of the electronic states with vibrational modes of the lattice mainly leads to more or less broad bands in the spectrum. Their half width FWHM is related to the Stokes shift S [Eqs (1a) and (1b)], that is the energy

$$\text{FWHM} = \sqrt{8 \ln 2} \sqrt{2 k T} \sqrt{S} \text{ [eV]} \quad (1a)$$

$$S = S_e \hbar \omega_e + S_g \hbar \omega_g \quad (1b)$$

difference between absorption and emission maximum (harmonic approximation and high temperature limit; usually already valid at room temperature when the same excited

state emits as is reached by absorption; S_e , S_g = Huang–Rhys parameter for the excited and ground state, respectively;^[3f] Figure 2).

Phosphors that show an emission with a large Stokes shift usually exhibit a low quenching-temperature, which is disadvantageous for many applications. Luminescent materials based on lanthanide ions circumvent this problem because the actual luminescent process is largely independent of its environment, a fact that makes them unique in the luminescence world. For example, for Eu^{3+}

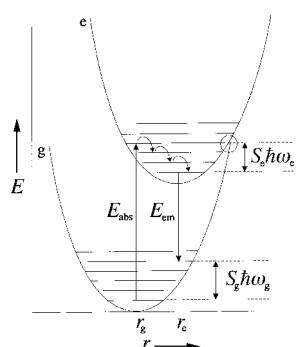


Figure 2. Potential energy curves illustrating an electronic transition from the ground to the excited state. The Stokes shift comprises of the terms $S_e \hbar \omega_e$ and $S_g \hbar \omega_g$.

activated phosphors such as $\text{Y}_2\text{O}_3:\text{Eu}^{3+}$ UV photons are absorbed through a charge-transfer state. In a consecutive step the energy is transferred to the f-niveaux, which are deactivated and show the characteristic f–f emission line spectra ($^5\text{D}_J \rightarrow ^7\text{F}_J$).

In general, the luminescent process can be divided into the steps of energy absorption, energy transfer, and emission. Energy absorption need not necessarily take place at the activator ion itself but can occur at a random place in the lattice. This implies that energy transfer of the absorbed energy to the luminescent center takes place before emission can occur. The migration of the energy absorbed by the lattice can take place through one of the following processes:

- migration of electric charge (electrons, holes),
- migration of excitons,

- resonance between atoms with sufficient overlap integrals,
- reabsorption of photons emitted by another activator ion or sensitizer.

The occurrence of energy transfer within a luminescent material has far-reaching consequences for its properties as a phosphor. On the one hand the absorbed energy can migrate to the crystal surface or to lattice defects where it is lost by radiationless deactivation. As a consequence the phosphor energy yield, that is the quotient of emitted light energy to initially absorbed energy, drops. Phosphors that emit UV, visible, or IR light upon UV excitation then show a decline in quantum yield QE [Eq. (2)]. Luminescent materials should be highly crystalline to achieve high light output, that is have as few lattice defects and impurities as possible. In addition, the surface area of the crystals has to be minimized, which means that their surface has to be clean and smooth.

$$\text{QE} = \frac{n(\text{emitted photons})}{n(\text{absorbed photons})} [\%] \quad (2)$$

On the other hand the use of sensitizers with the potential to considerably increase the light output of a phosphor is only possible because of energy transfer. For example, all Tb^{3+} -activated phosphors currently used in fluorescent lamps are sensitized with Ce^{3+} .^[2, 8] Tb^{3+} alone would absorb in most host lattices but at a wavelength shorter than 230 nm. UV photons with the main wavelength of 254 nm emitted by the mercury plasma in fluorescent lamps would therefore not be efficiently absorbed by the activator ion. Ce^{3+} , however, has a very high absorption coefficient between 250 and 350 nm and can effectively transfer the initially absorbed energy to Tb^{3+} .

Besides the quantum yield, the quality of a phosphor material is further characterized by its color point, the lumen equivalent, the reflection spectrum, and the emission lifetime under the given excitation conditions. The color point is derived from the spectral energy distribution of the emission and is defined according to the convention of the Commission Internationale d'Eclairage (CIE)^[9] in a normalized two-dimensional coordinate system.

From the color coordinates in the color triangle (Figure 3) not only the color itself but also the color saturation can be derived. The latter is most important for display applications (see Section 3) because in order to display all colors of the visible spectrum by synthesizing them from the three primary colors their respective colors have to be as saturated as possible, that is the color coordinates have to be positioned close to the borders of the color triangle.

For lighting applications the color saturation of the phosphors is of less importance. In contrast, the luminescent materials should emit a spectrum with a high lumen equivalent. This value is calculated^[9] by multiplication of the spectral power distribution $P(\lambda)$ of the phosphor emission, which integral has been normalized, with the spectral luminous efficiency for the human eye $V(\lambda)$ [Eq. (3), Figure 4].

$$\text{LE} = \int_{380}^{780} V(\lambda) P(\lambda) d\lambda [\text{lm W}^{-1}] \quad (3)$$

To obtain white light with a high lumen equivalent it is important that the phosphors applied in a mixture display very sharp emission spectra or, even better, emission lines

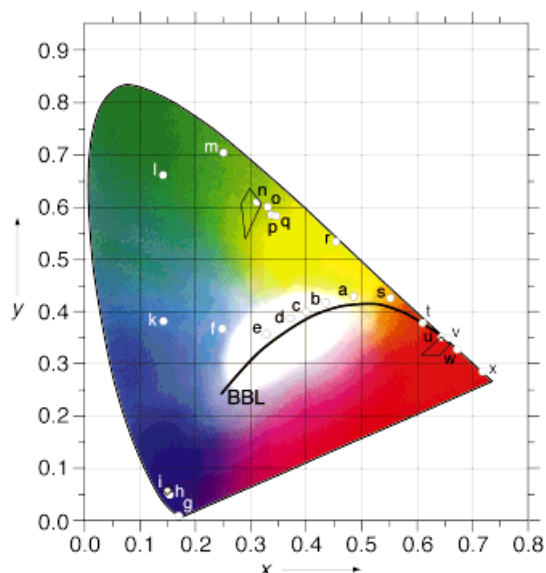


Figure 3. CIE color triangle showing the black body line (BBL) and the three EBU norm areas for cathode ray tube phosphors. The dots refer to the color points of the emission spectrum of the phosphor materials listed below. a)–e) Halophosphates with different color temperatures, f) blue emitting halophosphate, g) SPE, h) BAM, i) ZnS:Ag, k) SAE, l) BAM (green), m) ZSM, n) ZnS:Cu,Au,Al, o) CAT, p) LAP, q) CBT, r) YAG, s) SPS, t) CBTM, u) YOX, v) $\text{Y}_2\text{O}_2\text{S:Eu}$, w) YVE, x) MGM.

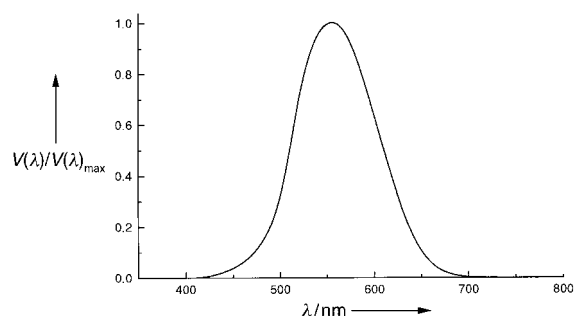


Figure 4. Normalized luminous efficiency for the human eye $V(\lambda)/V(\lambda)_{\max}$ as a function of the wavelength.

rather than broad emission spectra, otherwise light is generated in spectral areas where the eye sensitivity is too low. Naturally, also the emission maximum of line-emitting phosphors should not be too far off the eye sensitivity curve maximum.

Besides the quantity there is also a quality performance of light sources, with one factor usually being a trade-off against the other. Light quality is mainly determined by the color rendering of the light source, which is the ability to display the colors of an irradiated object in a natural way. A qualitative measure is the color rendering index (CRI), which by definition can adopt values between 0 and 100.^[9] This value is calculated by comparing the reflection spectra of selected test colors (either 8 or 14) obtained by irradiation with the light source under investigation with the reflection spectra when irradiated in the same way with a black body radiator. By definition a black body radiator like the sun or an incandescent lamp has a color rendering index of 100. In contrast, a line emitter with a single emission line at any part of the visible spectral region has a CRI of 0 because colors

cannot be displayed under such an irradiation source. This is illustrated on a late car ride, for example, on a Belgium highway that is continuously lit up at night with mostly low pressure sodium discharge lamps. This lamp type solely emits yellow light consisting of the sodium atom emission lines centered at 589 nm. It does not allow the perception of colors and thus turns the colored world into gray.

Discharge lamps that use phosphors for light conversion have CRIs between 50 and 95. The CRI of fluorescent lamps strongly depends on the applied phosphors. While a combination of line emitters yields high light output but moderate color rendering, broad band emitters enable higher CRI values to be obtained. In addition, color rendering is very dependent on the spectral position of the emission maximum and thus on the spectral power distribution of the applied phosphors. A compromise has to be found between color rendering and high light output.

3. Luminescent Lighting

Of all the artificially generated photons on earth 90 % originate from discharge lamps.^[10] All of today's efficient lighting sources are based on either direct or indirect light emission from plasma discharges. Most widespread is the application of mercury plasma because of its high energy conversion efficiency of about 75 %.^[11] In general, the spectral energy distribution of a plasma discharge depends strongly on the vapor pressure of the plasma gas inside the lamp tube. In low-pressure mercury discharge lamps the vapor pressure amounts to just a few torr, which results in a line spectrum with the main emission lines at 185, 254, and 365 nm. Further weak emission lines appear in the blue and green spectral region, and result in a faint blue–greenish glow of the plasma. Upon increasing the Hg pressure the emission lines broaden and finally collapse to yield an almost continuous spectrum between 250 and 550 nm. The visible part of the emission is used in high pressure mercury lamps operating at some 1000 torr. In both discharge types luminescent materials are needed to obtain white light with sufficient color rendering and efficiency.

3.1. High Pressure Mercury Discharge Lamps

To apply the light of the high pressure Hg plasma for general lighting purposes a color correction is necessary because the blue–greenish plasma light completely lacks the red spectral region and results in a low CRI of about 25.^[11] This tuning is achieved by introduction of a red emitting phosphor (Table 2) that has to absorb part of the UV and the

Table 2. Phosphors for the color correction in high-pressure Hg discharge lamps.

Phosphor	Abbreviation	λ_{\max} (em.) [nm]	λ_{\max} (ex.) [nm]	QE [%]	LE [lm W ⁻¹]
$\text{Mg}_4\text{GeO}_5\text{F:Mn}$	MGM	655	280, 420	80	80
$(\text{Sr,Mg})_3(\text{PO}_4)_2\text{:Sn}$	SPS	630	240	80	260
$\text{Y}_3\text{Al}_5\text{O}_{12}\text{:Ce}$	YAG	565	450	80	450
$\text{Y(V,B,P)O}_4\text{:Eu}$	YVE	615	255	85	225

blue–violet spectrum of the plasma. A further requirement on this phosphor material is a high emission-quenching temperature since the lamp tube can easily heat up to 300 °C. In the early 50s $\text{Mg}_4\text{GeO}_{5.5}\text{F:Mn}$ was the first phosphor to be introduced^[12] with a considerable increase in the CRI to 50. At the same time, the efficiency of the lamp decreased sharply for two reasons:

- The emission is located in the deep red spectral region where the eye sensitivity and, consequently, the lumen equivalent is very low.
- The phosphor absorbs both in the UV and blue spectral region, which takes away emission intensity in the useful spectral region.

This phosphor was later substituted by $(\text{Sr,Mg})_3(\text{PO}_4)_2\text{:Sn}$ with an emission maximum at 630 nm and therefore a higher lumen equivalent. Recently, $\text{Y(V,B,P)O}_4\text{:Eu}$ has been introduced as a line emitter with a very high lumen equivalent and high stability (Table 2). A disadvantage is the insufficient absorption of the vanadate group between 340 and 400 nm, which means that the UV emission of the Hg plasma is not completely absorbed and converted. As an alternative, $\text{Y}_3\text{Al}_5\text{O}_{12}\text{:Ce}$ with an intense 4f5d absorption at 460 nm might be used. However, its quantum yield is lower than in $\text{Y(V,B,P)O}_4\text{:Eu}$.

3.2. Low-pressure Mercury Discharge Lamps

Low-pressure mercury discharge lamps, better known as fluorescent or energy saving lamps, have penetrated the industrial and home lighting market to an impressive degree.^[11] This is easily explained by their high efficacy of almost 100 lm W^{-1} (white light), which amounts to about a 30% energy conversion efficiency and is about eight times as high as that of an incandescent lamp. A further advantage is the almost exclusive UV-light output of the low-pressure mercury plasma, which makes it possible to produce lamps with a spectrum dependent only on the phosphor mixture. This possibility means that a decoupling of the desired optical lamp features of the principal lamp construction is necessary since the lamp spectrum, the efficiency, and hence the application area is only determined by the phosphor mixture applied on the inner tube wall (Figure 5). This was a crucial factor for the success of this lamp type. Conventional fluorescent lamps as well as more advanced lighting applica-

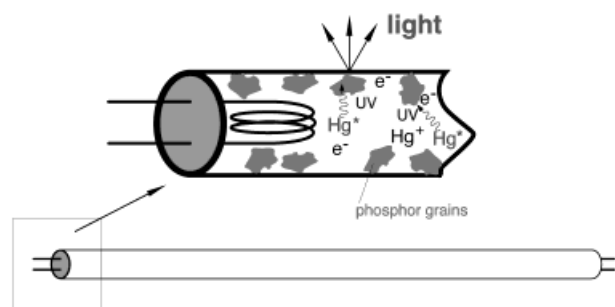


Figure 5. Schematic diagram of a fluorescent lamp illustrating the light generation process at the phosphor grains.

tions including for suntanning, photocopy machines, black-light, advertising billboards, display backlights, have been developed. Triggered by the large variety of areas of application some 50 different phosphors are currently produced for fluorescent lighting.

3.2.1. Halophosphate Lamps

To use low-pressure mercury discharge lamps for lighting applications, a phosphor had to be found to efficiently convert the UV light emitted from the plasma into white light. Since the early years of fluorescent lighting halophosphate materials with the composition $\text{Ca}_5(\text{PO}_4)_3(\text{F,Cl})\text{:Sb,Mn}$ (discovered in 1942) have been employed for this purpose.^[13] They emit both in the blue (Sb^{3+}) as well in the orange (Mn^{2+}) spectral region, thus in addition yield white light. However, the color rendering CRI of these halophosphate lamps reaches only 60–65 at an efficiency of about 80 lm W^{-1} . Variation of the Mn^{2+} to Sb^{3+} ion ratio in the host lattice allows the free adjustment of the color temperature between 2700 and 6500 K. With the halophosphates a white emitting material had been found to produce fluorescent lamps with sufficient efficiency and various color temperatures at very low cost. Consequently, the search for alternative broad-band phosphors was soon abandoned. Halophosphate lamps still have a considerable market share and today's focus in development is on improving the lifetime and reducing the color point shift that occurs during lamp operation. Both are caused by phosphor degradation and can be improved by closed inorganic coatings.

3.2.2. Tricolor Concept—Color 80 Lamps

After the theoretical treatment by W. A. Thornton, Opstelten and Koedam demonstrated in the early 70s that fluorescent lamps with very high color rendering and efficiency can be obtained if three narrow band emitters with emission maxima at 450, 540, and 610 nm are employed.^[14] These so-called tricolor lamps have color rendering CRI values of 80–85 at high efficiencies of 100 lm W^{-1} ! Figure 6 shows the emission spectrum of a typical fluorescent lamp employing $\text{BaMgAl}_{10}\text{O}_{17}\text{:Eu}$, $(\text{Ce,Gd,Tb})\text{MgB}_5\text{O}_{10}$ and $\text{Y}_2\text{O}_3\text{:Eu}$.

This new and clever concept triggered enormous research activities in both industry and universities in the field of

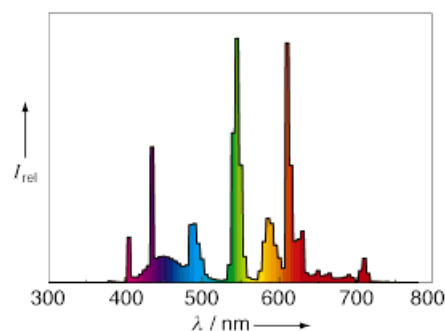


Figure 6. Emission spectrum of a tricolor fluorescent lamp.

lanthanide-activated phosphor materials. In particular Eu^{2+} -, Tb^{3+} -, and Eu^{3+} -doped host lattices were promising candidates because of their high quantum yields and spectral position of the emission, as described in numerous contributions.^[2, 15] Nevertheless, the material selection was accomplished relatively soon and until today only a small number of phosphor materials is being applied in the so-called Color 80 lamps (Table 3).

Table 3. Phosphors currently applied in Color 80 lamps.

Phosphor	Abbreviation	λ_{max} (nm)	Absorption at 254 nm [%]	QE [%]	LE [lm W^{-1}]
$\text{BaMgAl}_{10}\text{O}_{17}:\text{Eu}$	BAM	450	90	90	90
$(\text{Ce},\text{Tb})\text{MgAl}_{11}\text{O}_{19}$	CAT	541	95	90	495
$(\text{Ce},\text{Gd},\text{Tb})\text{MgB}_5\text{O}_{10}$	CBT	542	95	90	490
$\text{LaPO}_4:\text{Ce},\text{Tb}$	LAP	545	95	93	500
$\text{Y}_2\text{O}_3:\text{Eu}$	YOX	611	75	90	280

The luminescent materials used in today's tricolor lamps have both excellent quantum yields and absorption properties, in addition to high luminous equivalents. Consequently, it cannot be expected that phosphors with distinctly higher light output can be found in the future. During the last few years research has therefore focused on price reduction of phosphor materials. In particular the green emitting phosphor and $\text{Y}_2\text{O}_3:\text{Eu}$ are relatively expensive materials because of the high price of Tb, Eu, and Y minerals and the costly separation and purification of these lanthanides. The most effective price reduction in $(\text{Ce},\text{Gd},\text{Tb})\text{MgB}_5\text{O}_{10}$ would be achieved by lowering the Tb^{3+} dopant concentration, but this however at the same time effects the energy transfer from Ce^{3+} via Gd^{3+} to Tb^{3+} . Mn^{2+} activated materials like $\text{Sr}_3\text{Gd}_2\text{Si}_6\text{O}_{18}:\text{Pb},\text{Mn}$ ^[16] are discussed as cheap alternatives. Their drawback is a distinctly worse maintenance under lamp conditions than the Tb^{3+} phosphors $\text{LaPO}_4:\text{Ce},\text{Tb}$, $(\text{Ce},\text{Tb})\text{MgAl}_{11}\text{O}_{19}$, or $(\text{Ce},\text{Gd},\text{Tb})\text{MgB}_5\text{O}_{10}$ (Table 3). In addition, Mn phosphors are band emitters that, depending on the position and half-width of their emission bands, have much lower lumen equivalents than rare earth phosphors. Similarly difficult is the situation for $\text{Y}_2\text{O}_3:\text{Eu}$. Neither could the Eu^{3+} concentration of currently about 5 mol % be lowered nor have better host lattices been found, although a variety of materials such as $\text{BaGdB}_9\text{O}_{16}:\text{Eu}$,^[17] $\text{BiSr}_2\text{V}_3\text{O}_{11}:\text{Eu}$,^[18] or $\text{BaZrO}_3:\text{Eu}$ ^[19] show promising properties. However, no material so far was able to match "nature's gift", $\text{Y}_2\text{O}_3:\text{Eu}$. In this context, it will be exciting to watch the progress of combinatorial chemistry. Tens of thousands of combinations can be synthesized and evaluated on a single substrate wafer. A variety of often unusual phosphor materials has thus been identified by scanning libraries of even ternary systems.^[20] Recently, $(\text{Y},\text{Al},\text{La})\text{VO}_4:\text{Eu}$ has been found to have an efficiency close to commercial red phosphors.^[21]

Another approach for realizing cheap phosphor materials is the application of zeolites as host lattices.^[22] Low-cost materials such as zeolite X can be modified such that they do not absorb at wavelength longer than 240 nm, which is important for lamp application. These zeolites can be loaded

with Eu^{3+} or Tb^{3+} ions and indeed luminescing materials can be obtained, although only with low quantum yields and UV absorptions. The latter can be improved by employing organic sensitizers such as benzoate or inorganic transition metallates like MoO_4^{2-} .^[5] However, Eu^{3+} and Tb^{3+} zeolites still haven't exceeded quantum yields of 7 and 50 %, respectively. One reason for these low values are the high frequency O–H vibrations of the zeolites hydroxyl groups at the binding sites of the rare-earth metal ion which effectively quench the metal ion emission, especially from Eu^{3+} . An elegant way around this problem is to use zeolites as precursors for Eu^{3+} - or Tb^{3+} -doped aluminosilicates. Recently, this method allowed the simple synthesis of a quaternary aluminosilicate, $\text{EuMoAl}_2\text{Si}_4\text{O}_{16}$, with a quantum yield of 40 %.^[23]

3.2.3. Tricolor Lamps with High Lumen Output

Efficiency and color rendering of Color 80 lamps depend critically on the exact position of the emission maximum of the blue and red phosphor (Figure 7). $\text{Y}_2\text{O}_3:\text{Eu}$ with its main emission line at 612 nm is ideally suited for high color rendering. However, the luminous efficacy of fluorescent

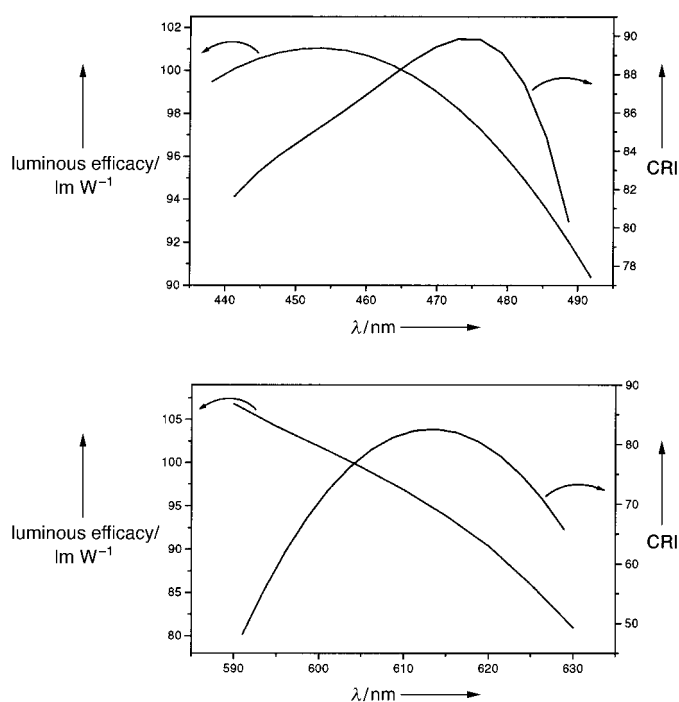


Figure 7. Luminous efficacy and color rendering index of a 36 W tricolor lamp as a function of the emission wavelength of the applied phosphor in the mixture. Top: Variation of the emission wavelength of the blue component. Bottom: Variation of the emission wavelength of the red component.

lamps can be further increased if the emission maximum of the red phosphor is shifted towards shorter wavelength and a decrease in color rendering is accepted. If the emission maximum of the red phosphor is shifted from 612 to 595 nm while leaving the green and blue phosphor unchanged, color rendering drops to 60–65 and the lumen efficiency increases by 12 % (Figure 7). This concept can be realized if $\text{Y}_2\text{O}_3:\text{Eu}$ is

substituted by another line emitter at 595 nm. Such a phosphor can be obtained with Eu^{3+} as the dopant in different host lattices. The electronic transitions of Eu^{3+} doped into host lattices with a trivalent lattice site with inversion symmetry are electronic dipole forbidden. As a consequence, the phosphor emission is mostly restrained by the $^5\text{D}_0$ – $^7\text{F}_1$ transition at 595 nm. Host lattices with a local inversion symmetry (for example D_{3d}) are InBO_3 , ScBO_3 , LuBO_3 (calcite structure),^[24] and $\text{BaYB}_9\text{O}_{16}$.^[16]

Compared to the $\text{Y}_2\text{O}_3:\text{Eu}$ “standard”, these now orange phosphors show indeed a considerably increased lumen equivalent of between 340 and 360 lm W^{-1} . Their quantum yields, however, do not reach the almost theoretically maximal value of $\text{Y}_2\text{O}_3:\text{Eu}$, which in consequence would compensate for most of the lumen gain. Materials with a quantum yield close to the $\text{Y}_2\text{O}_3:\text{Eu}$ benchmark have to be found in order to be successfully applied.

Recently, a new orange Eu^{3+} phosphor based on an $(\text{In,Gd})\text{BO}_3$ host lattice with a quantum yield of 90% has been developed. Its main emission lines are at 591 and 597 nm, which result in a lumen equivalent of 350 lm W^{-1} .^[25] In combination with $\text{BaMgAl}_{10}\text{O}_{17}:\text{Eu}$ and $(\text{Ce,Gd,Tb})\text{MgB}_5\text{O}_{10}$ (Table 3), a fluorescent lamp can be realized with about 7% more light output than with the classical tricolor mixture. The considerable emission intensity at 612 and 700 nm, which corresponds to the $^5\text{D}_0 \rightarrow ^7\text{F}_{2,4}$ transitions, is responsible for the deviation from the calculated 12% gain. It is questionable whether a phosphor can be found where these long-wavelength transitions are completely suppressed.

3.2.4. Color 90 Lamps

The tricolor lamps mentioned above employ line emitters that generate light in discrete wavelength intervals. Colored objects that absorb outside these spectral regions appear with a slightly different body color when illuminated with these lamps rather than with a black-body radiator such as a light bulb. This is acceptable for most applications such as general indoor and outdoor lighting. Special lighting areas such as museums and bay windows of stores demand a very natural appearance of illuminated objects. For this purpose, Color 90 or Deluxe lamps have been developed.^[8, 10]

Two measures serve to increase the color rendering of tricolor lamps. First, the emission maximum of the blue phosphor can be shifted towards longer wavelength (Figure 7). For example, substitution of $\text{BaMgAl}_{10}\text{O}_{17}:\text{Mn}$ with $\text{Sr}_4\text{Al}_{14}\text{O}_{25}:\text{Eu}$ yields lamps with a CRI of 90. Second, the red and green line emitters can be substituted by broad-band emitters covering the whole spectral range to yield even higher color rendering. For this concept, $(\text{Ce,Gd,Tb})\text{MgB}_5\text{O}_{10}:\text{Mn}$ has been developed as a red-band emitter; energy transfer from Ce^{3+} via Gd^{3+} to Mn^{2+} gives rise to an additional broad emission band at 630 nm.

Unfortunately, a green broad-band emitter with sufficient efficiency and stability is not yet known. However, an emission band in this region can be “simulated” by combining the green Tb line in $(\text{Ce,Gd,Tb})\text{MgB}_5\text{O}_{10}:\text{Mn}$ (Table 4) with the Mn^{2+} emission of $\text{Ca}_5(\text{PO}_4)_3(\text{F,Cl}):\text{Sb,Mn}$. With a phosphor mixture of $\text{Sr}_4\text{Al}_{14}\text{O}_{25}:\text{Eu}$, $(\text{Ce,Gd,Tb})\text{MgB}_5\text{O}_{10}:\text{Mn}$,^[26]

Table 4. Phosphors for Color 90 lamps.

Phosphor	Abbreviation	λ_{max} (nm)	Absorption at 254 nm [%]	QE [%]	LE [lm W^{-1}]
$\text{Sr}_4\text{Al}_{14}\text{O}_{25}:\text{Eu}$	SAE	490	90	80	270
$(\text{Ce,Gd,Tb})\text{MgB}_5\text{O}_{10}:\text{Mn}$	CBTM	630	90	80	215
$\text{Y}_3\text{Al}_5\text{O}_{12}:\text{Ce}$	YAG	565	45	80	450
$\text{Ca}_5(\text{PO}_4)_3(\text{F,Cl}):\text{Sb,Mn}$	Halo	585	90	80	390
$(\text{Ba,Sr,Ca})_2\text{SiO}_4:\text{Eu}$	BOSE	560	90	65	475

and $\text{Ca}_5(\text{PO}_4)_3(\text{F,Cl}):\text{Sb,Mn}$ a fluorescent lamp with a CRI of 95 can be obtained. As a trade-off, the emission intensity in the regions of low eye spectral response causes the lamp efficiency to drop to 65 lm W^{-1} .

Color 90 lamps with a low color temperature ($T_c < 3000$ K) demand a reduction in the intensity of the blue emission lines (405, 435 nm) from the mercury plasma. Fluorescent lamps of this kind employ a fourth phosphor with a relatively long-wavelength absorption, $\text{Y}_3\text{Al}_5\text{O}_{12}:\text{Ce}$.^[27] This material absorbs the blue–violet part of the spectrum very efficiently and converts it into a yellow emission at 565 nm.

$(\text{Ba,Sr,Ca})_2\text{SiO}_4:\text{Eu}$ has been developed as an alternative green-band emitter.^[28] Depending on its exact composition, the phosphor emits between 550 and 580 nm with a high quantum yield. Unfortunately, the host lattice is not stable in water, which prevents its deposition on the lamp bulb from aqueous suspensions and, for environmental reasons more and more lamp producers use water as the suspending solvent in production instead of butyl acetate.

3.2.5. Suntanning Lamps

Suntanning lamps have been in production for more than 30 years. Besides high pressure mercury discharge lamps that operate without the application of phosphor materials low-pressure mercury lamps in combination with phosphors have become increasingly popular. The degree of freedom of designing the (UV) lamp spectrum by the phosphor mixture (see Section 2.2) becomes an important feature here. A sensitive parameter for cosmetic, attractive tanning is the ratio of persistent (indirect) to immediate (direct) pigmentation of the skin. While UV-A (320–400 nm) radiation mainly induces immediate pigmentation, which results in a fast tanning and grayish brown color of the skin, UV-B (280–320 nm) radiation promotes the long-lasting, reddish brown tanning of the skin (Figure 8).^[10] Consequently, in the 70s the

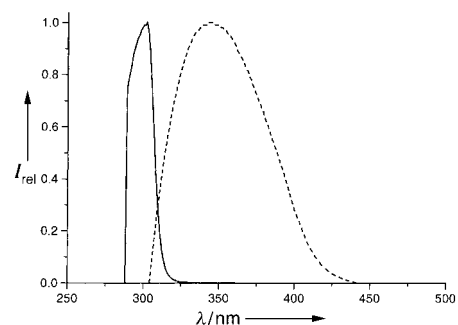


Figure 8. Persistent (solid line) and immediate pigmentation (dotted line) sensitivity of the skin in dependence on the wavelength of the incident UV light.

broad-band emitter $(\text{Sr,Zn})\text{MgSi}_2\text{O}_7:\text{Pb}$ (Table 5) was commonly used in suntanning lamps.^[29] This phosphor, which has its emission maximum at 365 nm with a half width of 70 nm, enabled a balanced UV-A/UV-B ratio and resulted in fairly good tanning. The main drawback of this material is its low

Table 5. Phosphors for suntanning lamps.

Phosphor	Abbreviation	λ_{max} (em.) [nm]	Absorption at 254 nm [%]	QE [%]	FWHM [nm]
$\text{SrAl}_{12}\text{O}_{19}:\text{Ce}$	SAC	310	85	95	34
$\text{BaSi}_2\text{O}_5:\text{Pb}$	BSP	350	85	95	38
$(\text{Sr,Zn})\text{MgSi}_2\text{O}_7:\text{Pb}$	SMS	365	88	85	70
$\text{SrB}_4\text{O}_7:\text{Eu}$	SBE	370	95	90	20

stability, which results in a low lamp maintenance. In addition, the large half width of the emission leads to considerable emission intensity beyond 400 nm where the skin sensitivity towards tanning and consequently the tanning effect is low (Figure 9).

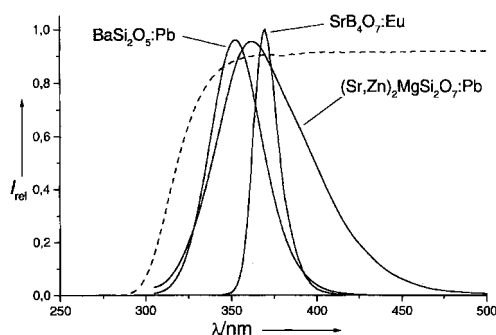


Figure 9. Emission spectra of the UV phosphors $\text{BaSi}_2\text{O}_5:\text{Pb}$, $\text{SrB}_4\text{O}_7:\text{Eu}$, $(\text{Sr,Zn})_2\text{MgSi}_2\text{O}_7:\text{Pb}$ applied in fluorescent tubes with a typical glass transmission (dashed line).

Besides these material-related shortcomings of $(\text{Sr,Zn})\text{MgSi}_2\text{O}_7:\text{Pb}$, scientific evidence gained in the 70s showed that UV-B radiation is responsible for direct damage of DNA. Such damage was not found for UV-A radiation. As a consequence, $\text{SrMgSi}_2\text{O}_7:\text{Pb}$ has been replaced by $\text{BaSi}_2\text{O}_5:\text{Pb}$ which emits at 350 nm with a rather small FWHM of the emission band. The emission intensity is now concentrated in the UV-A region, which speeds up direct pigmentation. Also, the UV-B emission intensity accumulated on the skin is lowered. Unfortunately, the persistent pigmentation which is long lasting, is decreasing at the same time.

However, in the 80s the booming suntanning industry focused on UV lamps emitting mainly UV-A radiation. The lowering of the UV-B/UV-A ratio was achieved by two measures. First, the glass transmission in the UV-B region was reduced. In addition, some manufacturers applied a second UV-A phosphor, $\text{SrB}_4\text{O}_7:\text{Eu}$ in a blend with $\text{BaSi}_2\text{O}_5:\text{Pb}$.^[30] The enhancement of the UV-A radiation of suntanning lamps was driven by the belief that tanning with UV-A is safe.

Since the early 90s photobiological investigations have revealed that UV-A radiation might also be responsible for inducing serious skin cancer, namely malignant melanoma.^[31]

These considerations and the demand to enhance the long-lasting tanning have recently led to the development of UV lamps with larger UV-B/UV-A ratios. Today, $\text{BaSi}_2\text{O}_5:\text{Pb}$ is typically used in combination with $\text{SrAl}_{12}\text{O}_{19}:\text{Ce}$.^[32] The introduction of this UV-B phosphor with an emission at 350 nm allows the fine-tuning of the UV-B to UV-A ratio.

Triggered by the discussion about health risks of suntanning, many lamp producers seek to further optimize the lamp spectrum. Positive effects of UV irradiation such as pigmentation, vitamin D production, epidermis thickening, and stimulation of the production of immunoglobulins can be enhanced by an accurate fine-tuning of the UV spectrum, while negative consequences such as photokeratitis, photoconjunctivitis, and photodimerization of pyrimidine bases should be lowered. Consequently, new phosphor combinations are tested as well as new phosphor materials that are developed to further improve the spectral power distribution of future suntanning lamps.

3.2.6. Specialties

Besides the discussed major application areas of low pressure mercury discharge lamps, a large variety of special lamps has been introduced into the market.^[2, 10] The development of these specialties was possible because phosphor materials with any emission spectra can be designed, which determine the spectral power distribution of the fluorescent lamp. Specialty lamps used in photocopy machines, billboards, plant illumination, skin disease treatment,^[33] for example, employ luminescent materials with emission spectra that serve the very special requirements of the respective application. Table 6 lists important applications together with the optical properties of the employed phosphors.

Table 6. Phosphors for specialty lamps.

Phosphor	Abbreviation	λ_{max} (em.) [nm]	Application area
$(\text{Gd,Lu})\text{B}_3\text{O}_6:\text{Bi}$	GLBB	311	psoriasis lamps
$\text{Sr}_2\text{P}_2\text{O}_7:\text{Eu}$	SPE	420	photocopy lamps
$\text{BaMgAl}_{10}\text{O}_{17}:\text{Eu,Mn}$	BAM-Mn	520	neon lamps
$\text{Mg}_4\text{GeO}_5\text{F}:\text{Mn}$	MGM	655	neon lamps, butcher lamps

3.3. Maintenance Improvement

Generally, phosphors show a decrease in efficiency during lamp operation. The maintenance of a material is defined as the relation of efficiency after a certain operation time, for example 1000 h, to the initial brightness of the virgin tube. The following processes have been identified to contribute to degradation:

- adsorption of Hg,
- sputtering of the phosphor surface by the plasma,
- solarization (staining) of the phosphor.

It is quite obvious that the phosphor degradation during lamp operation depends strongly on the chemical nature of

the material, that is the composition of the host lattice and the nature of the activator ion. For illustration, special host lattices such as silicates (e.g. Zn_2SiO_4) show a strong affinity to Hg.^[34] Adsorption of Hg onto the phosphor induces a complex chemistry that leads to surface defects of the phosphor grain or even the build-up of a Hg layer on the surface that consumes the mercury from the plasma. Redox-sensitive activator ions such as Mn^{2+} or Ce^{3+} easily undergo photochemical reactions such as photooxidation or -reduction. Solarization means the direct creation of defects in the phosphor grain by short wavelength UV light, which usually act as color centers that absorb UV- or visible light.

The loss of efficiency of a phosphor during lamp operation can be explained by the following processes:

- decrease of the UV absorption of the activator relative to the host lattice, that is, energy loss in the host lattice,
- drop of quantum yield because of energy transfer of the absorbed energy to so-called killer centers,
- increase of absorption of the emitted light in the single phosphor grain that leads to less light output of the phosphor (e.g. absorbing defects, photochemically generated absorbers),
- intrinsic quantum efficiency loss of the activator, for example by an oxidation or reduction process.

Phosphors with a good maintenance often consist of a host lattice with high chemical bond energies, for example $\text{Y}_2\text{O}_3\text{:Eu}$ or aluminates. However, the actual application of a phosphor material in lamps is the result of a thorough evaluation of optical performance and price, which means that less stable materials are also applied. In many cases, the maintenance of phosphors can be considerably improved if the surface of the phosphor particle is “finished” with a coating.^[4] The requirements of a coating material are stability and a high bandgap so that the incoming UV light is not already absorbed on the nonemissive coating surface. Typical materials are Al_2O_3 , Y_2O_3 , or La_2O_3 , which are commonly applied by precipitation from soluble precursors in aqueous solutions^[35] or by chemical vapor deposition (CVD).^[36] While the former procedure is a rather cheap one, the latter one is capable of producing very dense and homogeneously closed coatings. A variety of luminescent materials has been considerably improved by coating technology (Table 7).

Table 7. Examples of currently coated phosphors.

Phosphor	Coating material	Process	Benefit
$\text{BaMgAl}_{10}\text{O}_{17}\text{:Eu}$	Y_2O_3 or Al_2O_3	homogeneous precipitation	improved maintenance
$\text{Zn}_2\text{SiO}_4\text{:Mn}$	Al_2O_3	CVD	improved maintenance
$\text{BaSi}_2\text{O}_5\text{:Pb}$	Al_2O_3	CVD	improved maintenance applicable in water suspension
$\text{YVO}_4\text{:Eu}$	Y_2O_3 or Al_2O_3	CVD	improved maintenance
$\text{Y}_2\text{O}_3\text{:Eu}$	Al_2O_3	CVD	applicable in water suspension
$\text{Ca}_3(\text{PO}_4)(\text{F,Cl})\text{:Sb,Mn}$	Al_2O_3	CVD	reduced mercury consumption

Besides improved maintenance various other phosphor properties can be influenced positively. Lamp producers are increasingly applying phosphors from water-based suspensions (Section 2.2.3). Phosphors sensitive towards hydrolysis such as $\text{BaSi}_2\text{O}_5\text{:Pb}$ and $\text{Mg}_4\text{GeO}_5\text{:F:Mn}$ could then not be applied. However, both materials can be coated quite well by CVD and thus be adapted to the new process technology. Coatings can also help to reduce the mercury consumption by the phosphor surface and the color point shifts of the phosphor during lamp operation.^[37]

In summary, the maintenance improvement of luminescent materials is of increasing importance for phosphor producers. Particle coatings and the development of new coating processes improve both the applicability and stability of luminescent materials.

3.4. Alternative Discharge Types and Quantum Cutters

The overall efficiency of low pressure mercury discharge lamps ϵ_{lamp} is close to 30 %. The value is mainly determined by the efficiency of the mercury plasma (75 %), the energy loss from the conversion of UV light into visible radiation, and the quantum efficiency of the employed phosphors [Eq. (4)].

$$\epsilon_{\text{lamp}} = \epsilon_{\text{discharge}} [\lambda_{\text{UV}}/\lambda_{\text{vis}}] \text{QE} \quad (4)$$

Mainly for environmental reasons, alternative plasma discharges that could substitute the mercury plasma are widely investigated today. With regard to discharge efficiency, a xenon excimer plasma is the most promising candidate, with an efficiency of up to 65 % reported recently.^[38] A Xe discharge is also used in plasma display panels (PDPs) (Section 4.2.2). The main emissions are in the vacuum ultra-violet (VUV) at 147 (Xe fundamental line) and about 172 nm (Xe excimer band) and their ratio depends on the gas pressure in the discharge cell. Since they are at shorter wavelengths than the mercury plasma emission the overall efficiency of visible light generation is reduced because of the now much bigger energy gap between the excitation and emission levels. A scientifically quite exciting solution to this problem are phosphors that emit in a controlled way more than one visible photon per absorbed VUV photon. Such materials, so-called quantum cutters, were reported for the first time in the mid 70s independently by two research groups.^[39] In the phosphors $\text{YF}_3\text{:Pr}$ and $\text{NaYF}_4\text{:Pr}$ the Pr^{3+} activator ion can be excited by a VUV photon into the very energy rich $^1\text{S}_0$ state. From there it can emit in a photon cascade emission (PCE) two visible photons of different energies. The initial absorption takes place in the host lattice at 185 nm via a $4f5d$ transition. It is important that the excited $4f5d$ state lies above the $^1\text{S}_0$ state so that energy transfer can lead to the excited $^1\text{S}_0$ state. Only if this condition is fulfilled can the two f-f states of Pr^{3+} be populated and emit with a combined quantum yield of about 140 %. If the $5d$ state moves close to or below the $^1\text{S}_0$ state, as in $\text{LiYF}_4\text{:Pr}$ or $\text{YPO}_4\text{:Pr}$, quantum cutting cannot be observed anymore. This is the case in host lattices with a strong crystal

field. Unfortunately, fluorides have pronounced disadvantages that have so far prevented their application. They are difficult to handle in production and show a poor maintenance in contact with plasma discharges. Consequently, research focuses now on alternative host lattices such as oxides, aluminates, or borates. Oxide anions create a stronger crystal field than fluorides, however, it can be weakened by a large coordination number. Recently, this concept has been realized successfully by Shrivastava et al. in several Pr^{3+} -doped host lattices with a coordination number of 10 or 12, for example $\text{SrAl}_{12}\text{O}_{19}$,^[40] LaB_3O_6 ,^[41] and $\text{LaMgB}_5\text{O}_{10}$.^[42] Photon cascade emission has been observed; however, as a consequence of the very low transition probability in these hosts, the external quantum yield does not exceed 100%. Another drawback of Pr^{3+} quantum cutters is their emission spectra, which consists of two major emission lines at 610 and 410 nm, the latter of which is not very useful for fluorescent lamps because of low color rendering and efficiency (Section 3.2.3).

A few month ago Meijerink et al. presented a completely different quantum cutter concept based on the material $\text{LiGdF}_4:\text{Eu}$.^[43] This system is particularly attractive because it yields solely “useful” Eu^{3+} emission at 612 nm with a demonstrated internal yield of 195%. A VUV photon is absorbed by the Gd^{3+} sensitizer and then transferred in two steps to a Eu^{3+} ion. In a first step the Eu^{3+} ion is excited by cross relaxation while in the second step another Eu^{3+} ion can be populated by energy transfer from Gd^{3+} to Eu^{3+} ions (Figure 10). Although again based on a fluoride host lattice,

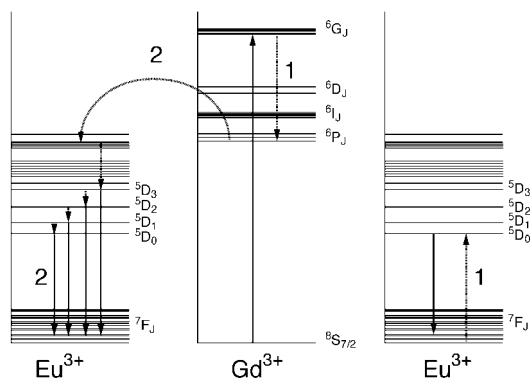


Figure 10. Energy level scheme of the quantum cutter $\text{Li}(\text{Gd},\text{Y})\text{F}_4:\text{Eu}$ showing the transitions 1 and 2, which lead to emission of two photons.^[43]

this material and the concept behind it might open new ways to realize quantum cutting with useful emission in novel lamp applications.

3.5. Light Emitting Diodes in Comparison and in Combination with Luminescent Materials

The invention of the blue-light emitting diode (LED) based on GaN can be regarded as a triumph of material chemistry. Electroluminescence based on III–V nitride semiconductors had already been abandoned when S. Nakamura picked up the topic again in the late 80s and developed it within only 5 years to an impressive level of maturity. Excellent reviews

about the underlying semiconductor photophysics as well as the MOCVD technique used for LED chip production can be found elsewhere.^[44, 45] External quantum yield, stability, and many other favorable properties of this material class allow even the construction of the blue laser diode, which will likely revolutionize the storage capacity of compact discs. Very recently, lifetimes exceeding 10000 h have been reported, which paves the way for a fast introduction of the blue laser into the market.^[46] The blue diode itself however might already mark the beginning of a slow revolution of the lighting market. External efficiencies of close to 10% have already been achieved. Light outcoupling from the LED chip into the epoxy dome as well as the chip architecture still show considerable room for improvement, so much higher efficiencies seem possible. By varying the In content of the InGaN active layer the emission spectrum of GaN LEDs has successfully been extended into the green spectral region with still high efficiencies. As a consequence, for the first time it is possible to generate white light by direct conversion from electrical current in LEDs with an efficiency superior to halogen lamps. Two ways of generating white light appear likely. First, blue, green, and red diodes can be combined to yield white light. So-called cluster lamps consisting of blue, green, and red LEDs are already on the market. Second, in a very cheap way a single white LED can be obtained by combining a blue LED with green, yellow, and/or red emitting phosphor materials that absorb and convert part of the incident blue light. In comparison to the three LED device this causes a decrease in the overall efficiency because the quantum deficit of the light conversion from blue to yellow/red has to be taken into account. In the following paragraph this option will be discussed with regard to light quality and luminous efficiency.

In principle, it is possible to vary the emission wavelength of blue GaN-based LEDs between 370 nm, which marks the bandgap of pure GaN, and 470 nm by increasing the In content in InGaN devices. Assuming a conversion from the incident light by a phosphor material emitting at 555 nm (a spectral “mean value” for white light), the already mentioned quantum deficit decreases in the same direction from about 33% to 15%. The more favorable option is therefore a combination of a blue LED emitting at 470 nm and a broad-band phosphor that can be excited by that wavelength and reemits at about 550 nm to create white light composed of the blue and yellow–green emissions. Such a device has been realized by using $(\text{Y}_{1-x}\text{Gd}_x)_3(\text{Al}_{1-y}\text{Ga}_y)_5\text{O}_{12}:\text{Ce}$ (YAG:Ce) as a broad-band yellow phosphor (Figure 11).^[44] The variation of x and y causes a shift of the YAG:Ce emission between 510 and 580 nm. This allows the adjustment of white color temperatures from 8000 down to 3000 K. A color temperature of 6000 K has been chosen for commercialization in the Japanese market, which demands high color temperatures. As a consequence of the broad YAG:Ce emission the color rendering index (CRI) is high and reaches a value of 85. The luminous efficiency is 5 lm W^{-1} , which is already half of that of an incandescent lamp. This shows clearly the potential of the blue LED and its importance for the future lighting market. All low-power white-light sources that demand long lifetimes could possibly be replaced by white LEDs in the

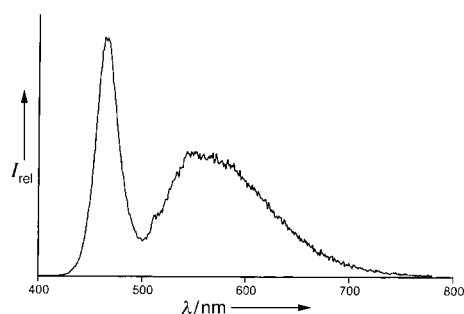


Figure 11. Emission spectrum of a white phosphor LED that consists of a blue LED that excites the YAG:Ce phosphor deposited as a thin layer on the LED chip.

medium term. However, it should be pointed out that about 80 such LEDs are still necessary to replace a 10 W light bulb, assuming a medium power operation of 50 mA at 5 V. The major drawback of this combination is the strongly decreasing overall efficiency upon lowering the color temperature. This is caused by the broad YAG:Ce emission, which shows less and less integral overlap with the eye sensitivity curve when shifted towards longer wavelengths (Figure 4) and hence decreases the luminous efficacy. Alternatively, pure organic perylene based materials (Lumogen dyes)^[47] and light emitting polymers^[48] can also be used for color conversion. Their advantage is the high absorption of the blue diode light. The white light energy yield achieved, however, is lower than for the YAG phosphor. An attractive alternative to the discussed broad-band phosphor systems would be the employment of line emitters in analogy to lamp phosphors (Section 2). The requirements can be concluded from the above discussions. The phosphor material has to have a sufficient absorption at the emission wavelength of the blue diode, the quantum yield should be high under UV/Vis excitation and the FWHM of the emission band should be as small as possible in order to achieve high luminous output. Selected rare-earth phosphors based on Eu^{3+} and Tb^{3+} fulfill the latter two options; however, there is a theoretical low energy limit for the maximum wavelength of the excitation peak. Even if tight sensitization schemes can be found, that is sensitizers with energy levels close to the ^5D terms of Eu^{3+} and Tb^{3+} , these ions cannot be excited with peak wavelengths longer than 420 and 370 nm, respectively. This is a result of the downward energy cascade that is necessary to effectively sensitize the rare-earth ion without back energy transfer.^[49] GaN LEDs that emit at 370 nm (see above) could be used for excitation with the drawback of the larger quantum deficit.^[50] Inorganic Eu^{3+} phosphors with high quantum efficiencies that absorb satisfactorily at 370 nm are $\text{Y}_2\text{O}_2\text{S}:\text{Eu}$ and $\text{Y}(\text{V,P,B})\text{O}_4:\text{Eu}$. Tb^{3+} -doped materials are hard to find; $(\text{Ce,Tb,Gd})\text{MgB}_5\text{O}_{10}$, mainly used in tubular fluorescent lamps, absorbs only to about 10% at 370 nm. Organic phosphors employing Eu^{3+} and Tb^{3+} coordinated to light-absorbing organic ligands can be designed to absorb efficiently at 370–400 nm.^[51] However, stability and saturation issues have yet to be improved for these materials. Despite these difficulties and the higher quantum deficit, a LED emitting UV light at 370 nm covered with a rare-earth phosphor mixture would be an attractive option from a production point of view. In contrast to a

phosphor deposited on a blue emitting LED chip at 470 nm, which only partly absorbs the blue light in order to generate white, a mixture of blue, green, and red phosphors on a UV LED absorbs all of the incident light emitted by the chip. The white light color coordinates are determined only by the phosphor portions in the mixture (see Section 3.2), which can be adjusted rather accurately. Consequently, white LEDs can be produced with color coordinates that vary only very little from LED to LED. This is considerably more difficult for a LED where white light is composed from incident blue emission from the diode and yellow/red light emitted by the phosphor. Deposition of a well-defined phosphor layer on the LED chip of some 1 mm² to achieve controlled absorption means a real manufacturing challenge. Further, the additional quantum deficit of about 15% of a color conversion from 370 nm relative to 470 nm can be compensated for considerably by the very high lumen equivalents of Eu^{3+} - and Tb^{3+} -activated phosphors. By analogy to fluorescent lamps (see above), high color renderings can be obtained at the same time. The search for stable inorganic rare-earth phosphors with high absorptions in the near UV/blue spectral region is therefore an attractive research task.

4. Displays

4.1. Cathode Ray Tubes and Projection TV

The classical cathode ray tube (CRT) invented as the Brown tube more than 100 years ago has developed into a remarkably mature product considering the complexity of its manufacturing process. An illustrative example is the deposition of the phosphor material on an average-sized, warped (!) screen front: In three consecutive photolithographic steps more than one million phosphor dots less than 300 μm in diameter for each color have to be deposited, with not one final pixel missing. Today's mass production, which yields more than 100 million tubes per year, has caused the prices to drop to a level where it is hard for innovations to step in. On the other hand, it is this number that makes research on CRT phosphors still a respectable field as they contribute a total of only about 2 g (red, green, and blue, average tube size), which is only very little, to the product. The strong competition drives the research effort on luminescent materials into two directions, namely cheaper phosphors (especially red) and the addition of new features for superior performance. Basic requirements of display phosphors are stability (20000 hours operation) and emission color purity according to the standards set by the European Broadcasting Union (EBU).^[2, 52] Color purity can be visualized in the chromaticity diagram as blue, red, and green regions, which the emission color coordinates of the luminescent material have to match (Figure 3). The blue and green phosphors are still the very cheap ZnS based materials, essentially the same ever since color TV was introduced in the 50s. The luminescence of both is based on donor–acceptor transitions in the ZnS host lattice that is doped with some 200 ppm Cl^- ions as donor and Ag^+ ions as acceptor for blue and Cu^+ ions, Au, Al for green.^[53] Remarkably enough, these sulfidic lattices are quite stable

towards electron beam excitation of 30 keV where one electron can create up to 3000 visible photons in the phosphor grain. The energy density of this excitation source has been described very graphically by H. A. Klasens, a pioneer in luminescent materials: “ultraviolet excitation compares to striking one key of the piano, cathode-ray or X-ray excitation compares to throwing the piano down the stairs”.^[2] This stability is not a natural property as we can see for low-voltage excitation (see below). Originally, a ZnS based host lattice containing a certain amount of Cd doped with Ag⁺ and Cl⁻ ions was used as the red phosphor. Intrinsic to a donor–acceptor transition, it displays a broad emission, in this case centered at 650 nm, which leads to a rather low lumen equivalent because a large fraction of the emission integral lies outside the eye sensitivity curve (see Section 2). For this and environmental reasons, it has been replaced by the much more expensive Y₂O₂S:Eu (a line emitter such as Y₂O₃:Eu) with main emission lines at 612 and 628 nm.

Key features of a modern CRT within a computer monitor or a TV set are brightness and contrast. The relation between the two is expressed by the luminance (L) contrast performance (LCP) gain [Eq. (5)], where R is the reflection of ambient light at the phosphor layer.

$$\text{LCP} = L/\sqrt{R} \quad (5)$$

From the equation two ways for improving LCP can be derived:

- increasing L , which is hardly possible anymore as all three phosphors are operating close to their physical limits, or
- reducing R , which is achieved by applying color filters and absorbing the ambient light while transmitting the light emitted by the phosphor.

Color filters can be applied by two means. Externally, as transparent layers on the screen glass or internally, as pigment on the phosphor surface. Pigmenting blue and red phosphors is the focus of CRT phosphor research these days. The phosphor grain is coated with nanosized pigments in the order of 100 Å such as α -Fe₂O₃ (red) and CoAl₂O₄ (blue) by a wet-chemical process. Figure 12 shows the absorption edges of the two pigments together with the emission bands of ZnS:Ag,Cl and Y₂O₂S:Eu. The green phosphor is not coated because calculations show that least LCP can be gained here and because no appropriate pigment can be found. It is easy to imagine that pigmentation changes the phosphor grain surface considerably and will consequently alter the phosphor suspension behavior in the industrial coating process. Also, pigment absorption can hamper the photolithographic deposition. The materials under development have to be adapted such that the industrial deposition techniques have to be changed as little as possible.

Projection TV (PTV) has a long history as well. Interestingly, the first color television developed in the 50s can be regarded as a projection TV. Requirements of projection TV phosphors are different.^[2, 54] PTV is used for large screen sizes (>90 cm) or in special environments like planes. Three monochrome (red, green, and blue) images are projected and superimposed on a screen at a certain distance. The need for high light output and resolution causes higher excitation density at a smaller phosphor volume than in a conventional

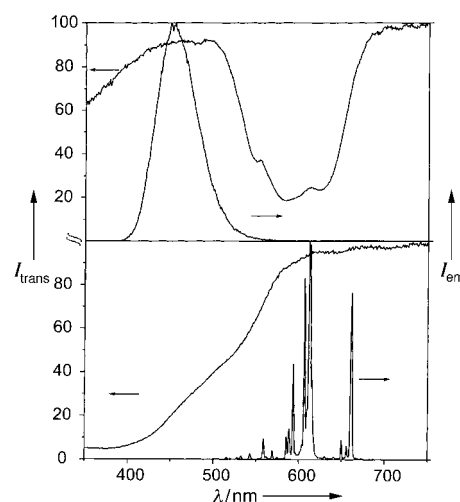


Figure 12. Color filter concept in cathode ray tubes. Emission and transmission spectra of the blue ZnS:Ag phosphor in combination with a CoAl₂O₄ filter (top) and the red Y₂O₂S:Eu phosphor in combination with a Fe₂O₃ color filter (bottom).

cathode ray tube. Most of the phosphor materials start to behave nonlinearly under these conditions, that is they don't increase light output L linearly upon increasing excitation density D [Jcm⁻²pulse⁻¹]. Saturation and heat-up of the phosphor grains up to 100 °C are the responsible factors. The former is the reason for switching from Y₂O₂S:Eu to the fluorescent lamp phosphor Y₂O₃:Eu, which is much less susceptible to saturation. As a green phosphor Y₂SiO₅:Tb is mostly used. The limiting phosphor and consequently research topic for a long time is the blue one. Introducing blue lighting phosphors (Section 3) does not work because all Eu²⁺-based materials suffer from severe degradation. Quite some effort, also in our lab, has been put into (La,Gd)OBr:Ce because of its good linear saturation behavior,^[55] however, without reaching industrial maturity. Once again, ZnS:Ag,Cl is used as the blue phosphor, despite saturation at high excitation densities. However, the triumphant march of LCD technology might also displace phosphor screens. Newly developed, extremely powerful high-intensity discharge lamps can project images from three tiny, monochrome high-resolution LCD screens and superimpose them in analogy to images projected from phosphor screens.^[56]

4.2. Flat Displays

The race for the flat screen has already begun. The big electronic companies are trying to enforce the ultimate display concepts for the respective application. For the smaller screen sizes up to 21" (monitors) it will be most likely liquid crystal technology (LCD). As a nonemissive display, it will not be covered in the following sections; excellent reviews can be found elsewhere.^[57] Various concepts exist for larger sizes up to 42" and beyond (>1 m diagonal) for TV application. Besides the one screen principle, which also uses LCD technology and the so-called plasma-addressed liquid crystal (PALC) display, all of the methods create light from

luminescent materials and are presented below. Very new developments such as electroluminescence, both organic and inorganic, conclude this chapter.

4.2.1. Low Voltage Displays

Electrons accelerated by moderate voltages between some hundred volts and 8 kV (compared to about 30 kV for a CRT) are used for excitation in this display type. Most prominent are the flat CRT and field emission displays (FEDs). The flat cathode ray tube was a large research project within Philips, which had achieved an impressive maturity level.^[58] It was aimed at medium to large sizes of screens to replace the bulky CRT by a hang-on-the-wall TV. Electrons are created at a flat cathode, the so-called backplate, and tunnel through a smart array of channels to arrive at a selection plate where they are distributed to address the phosphor pixels consisting of blue, green, and red phosphor dots.

The now very small distance between the back and front plate is filled with the channel plates and allows an acceleration voltage of only 4–6 kV in order to prevent shortcuts. $\text{Y}_2\text{O}_2\text{S}$, the red CRT phosphor, can be excited very well under these conditions. The green and blue ZnS phosphor, however, show a very fast degradation if excited this way. At a first glance, this seems rather surprising as less energy-rich electrons than in CRTs are used for excitation. The explanation is given in Figure 13. In contrast to high acceleration

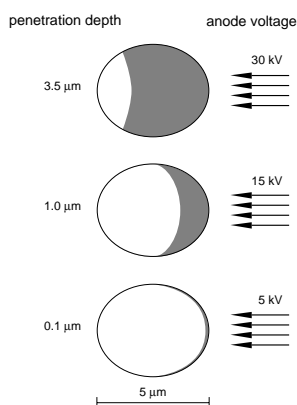


Figure 13. Dependence of the penetration depth of the electron beam in a phosphor grain of 5 μm diameter on the anode voltage of a cathode ray tube.

voltages, low-voltage electrons are not capable any more of penetrating the whole phosphor grain with an average diameter of about 5 μm . Instead, they create a high density surface excitation. This has physical and chemical consequences. The decreasing number of luminescent centers available for excitation at decreasing anode voltages results in severe phosphor efficiency saturation, even more as the energy density of excitation has to be increased in order to obtain a screen luminance comparable to a conventional CRT. Further, one of the main emission quenching pathways in a phosphor grain is formed by lattice defects that occur mostly at the surface. Low voltage surface excitation is therefore

more strongly quenched than excitation taking place in the bulk phosphor grain. The saturation effect in the low-voltage excited region compares well to PTV excitation. For this reason, the green $\text{Y}_2\text{SiO}_5\text{:Tb}^{3+}$ phosphor used there (see above) has been successfully adapted and has replaced ZnS:Cu for low-voltage excitation.

In addition to these photophysical loss processes chemical degradation occurs in ZnS phosphors upon low-voltage excitation. Although the detailed reaction path is still not completely understood, the sum reaction is believed to be sulfur loss in the host lattice caused by oxidation of sulfide anions, which create new quenching centers at the surface.^[59] Again, it is hard to find a more effective blue CRT phosphor than ZnS:Ag. As a consequence, efforts to develop a protective coating to prevent the fast degradation of ZnS:Ag under low voltage excitation have replaced the search for new materials. Inorganic coatings have been found, which form a completely closed, smooth, and only 20 nm thick layer on the surface. The so-called coulomb degradation is drastically reduced for coated ZnS:Ag. Most likely, the dense coating acts as a diffusion barrier and so maintains the sulfur balance within the host lattice.

Field emission display research is mainly conducted in the U.S. The display principle is similar to the flat CRT discussed above.^[60] Instead of an electron transfer mechanism through channels, electrons in FEDs are created at micro-tips which act as tiny cathodes. Each cathode addresses a pixel on the front plate that is mounted at a certain distance from the tips on the backplate. The voltages in FEDs are typically somewhat lower than in the flat CRT, ranging from some 100 V to a few kV. The low voltage phosphors applied in the flat CRT can still be used in FEDs, however, it can easily be concluded from the above discussion that because of the lower voltages degradation problems become even more severe. Oxidic host lattices would be favorable, however, they lack efficiency. The phosphors commonly applied today can be seen in Table 8.

Table 8. Overview of currently applied FED phosphors.

Phosphor	Efficacy ^[a] [lm W ⁻¹]	Color coordinates ^[a]		Color
		x	y	
SrTiO ₃ :Pr	0.4	0.670	0.329	red
Y ₂ O ₃ :Eu	0.7	0.603	0.371	
Y ₂ O ₂ S:Eu	0.57	0.616	0.368	
Zn(Ga,Al) ₂ O ₄ :Mn	1.2	0.118	0.745	green
Y ₃ (Al,Ga) ₅ O ₁₂ :Tb	0.7	0.354	0.553	
Y ₂ SiO ₅ :Tb	1.1	0.333	0.582	
ZnS:Cu,Al	2.6	0.301	0.614	blue
Y ₂ SiO ₅ :Ce	0.4	0.159	0.118	
ZnGa ₂ O ₄	0.15	0.175	0.186	
ZnS:Ag,Cl	0.75	0.145	0.081	

[a] At low-voltage excitation.

The white light generation efficiency is still well below 5 lm W⁻¹, which can already be achieved with LCDs. However, FEDs have other distinct advantages such as a very wide range of operational temperatures, they can operate under rugged conditions, and the emissive character results in a wide viewing angle. FEDs in the current status are mainly targeted towards military applications.^[61] Recently, a display based on

an alternative cathode structure has been realized, a so-called surface-conduction electron emitter display (SCE).^[62] This system consists of a structured PdO film that can easily be ink-jet printed. It operates at higher anode voltages (6 kV) and standard CRT phosphors were applied successfully. The performance of a 10" prototype (luminance 690 cd m^{-2} ; efficiency 5.3 lm W^{-1}) is well beyond that of "classical" FED concepts, not least because many phosphor problems have been overcome by the higher excitation energy.

4.2.2. Plasma Displays

Creating light from a plasma discharge ignited in the discrete display pixels is actually a rather old invention (the first laptop display was based on a plasma discharge). However, some years ago improved yields and refined production techniques have revitalized the principle. Today, all major electronic companies are conducting research on PDPs and mass production started about one year ago. The principle is sketched in Figure 14.^[63] A discharge is ignited between two electrodes in each pixel cell at the front plate that are filled with a Xe gas mixture to lead to a Xe plasma. Excited Xe monomers and excimers are formed that emit at

147 and 172 nm, respectively (Section 3.4). This light excites the phosphor layer on the wall of the discharge cell. As a consequence of the cell geometry, the discharge efficiency is rather low (about 6%), which is the major drawback of this display type. Currently, only about 1 lm W^{-1} screen efficacy (white light) is achieved compared to about 3 lm W^{-1} for a conventional CRT. This puts pressure on the phosphors for maximum performance.^[64] For blue, $\text{BaMgAl}_{10}\text{O}_{17}:\text{Eu}$ is mostly used because it can be excited very effectively. However, it shows degradation under VUV excitation, which might possibly be prevented by coatings. For green, the long known $\text{Zn}_2\text{SiO}_4:\text{Mn}^{2+}$ phosphor (willemite) is used because its green emission color is very saturated (color coordinates: $x = 0.250$, $y = 0.704$; see Figure 3). However, the optical transition within the Mn dopant is of the d–d type and thus a strongly forbidden electric dipole transition. As a consequence, the decay time is rather long, typically tens of milliseconds. It would exclude this material from TV application because for fast moving pictures, for example during a soccer game, a green afterglow would always be blurring the displayed image. Interestingly, magnetic interactions between pairs of Mn^{2+} ions^[65] can alter the transition probability. Thus, by increasing the concentration of the Mn^{2+} dopant the decay time starts to drop while the quantum efficiency is maintained.^[66] But at rather high concentrations of the activator concentration quenching causes the quantum efficiency to drop. This unique effect could be exploited to obtain a material that can be applied in PDPs. As a red phosphor, $(\text{Y}, \text{Gd})\text{BO}_3:\text{Eu}$ is mostly applied today. Borates have much higher VUV absorptions than for example $\text{Y}_2\text{O}_3:\text{Eu}$ does. However, because of the high symmetry of the trivalent site in the borate host lattice the $^5\text{D}_0 \rightarrow ^7\text{F}_1$ transition of the Eu^{3+} ion at 595 nm becomes very pronounced. This leads to a too orange color point according to the CIE standards. Obviously, the introduction of a functioning red quantum cutter phosphor (Section 3.4) would boost the overall PDP performance considerably.

4.2.3. Electroluminescence

Analogous to LED light sources, electroluminescence (EL) displays means the direct transformation of electrical current into light. It can be cautiously stated that if at all, only EL is possible to challenge the very mature LCD technology omnipresent in today's notebooks and flat monitors. Inorganic and organic EL are very different. Inorganic EL has been studied for some 30 years and is already used, for example as information displays in the new ICE trains. Organic EL is a very recent discovery and will have to prove its potential yet.

Electroluminescent Inorganic Materials

In this section new developments in materials for thin film alternating current electroluminescence (ACFEL) will be presented. Based on this principle, very thin full-color displays can be realized (with a thickness of a few centimeters, including the necessary electronics).^[67] Full color ACFEL displays are based on one of the two principles:

- Color by white: Here, white light is generated by a phosphor (a multilayer of $\text{ZnS}:\text{Mn}/\text{SrS}:\text{Ce}$). Color is

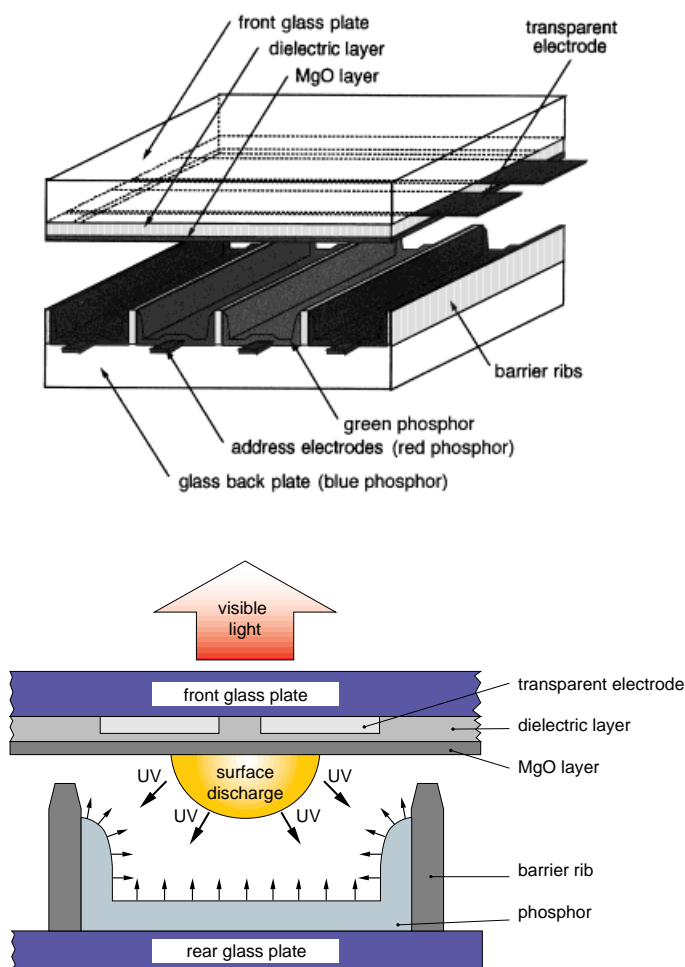


Figure 14. Top: schematic diagram of a plasma display panel. Bottom: cross-sectional view of a single plasma discharge cell illustrating the process of light generation

generated by the application of color filters. This principle has the advantage of a simple layer structure of the phosphor.

- Three color structure: In this principle, white light is generated by the application of three phosphors (emitting blue, green, and red, such as in a cathode ray tube). The phosphor layer structure and hence device fabrication is more difficult than in the color by white structure. In addition, for blue and red the color points of the emission spectrum are not fulfilling the EBU requirements. Therefore, also in this case, color filters are used. Nevertheless, these devices have a higher luminous efficacy than the ones based on the color by white structure (see below).

The following device structure is common to both principles:

glass substrate/electrodes/insulator/phosphor/insulator/electrodes/color filters.^[68]

The luminescent materials applied are thin layers (in the order of 1 μm), generated by techniques like atomic or molecular beam epitaxy. The electroluminescent materials applied are sulfides, although oxides are under investigation as well. The ACTFEL materials are subjected to high fields and electrons are accelerated in these materials. The electrons excite the activator ions by impact excitation. At present, there is no general picture of the mechanism(s) underlying ACTFEL. One of the most important factors determining the success of ACTFEL is the device efficiency, an estimation of which^[4] follows in brief below. The maximum efficiency η is given in Equation (6), where E_{em} is the photon energy of the emitted radiation, σ the cross-section for impact excitation, N the optimum concentration of luminescent centers, and F the electric field applied. $(\sigma N)^{-1}$ is the mean distance that an electron travels through the luminescent material between two excitation events.

$$\eta = E_{\text{em}} \sigma N / eF \quad (6)$$

The cross-section is not known a priori. In the case of ZnS:Mn (the most efficient ACTFEL material known) we approximate it by using atomic dimensions, that is $\sigma = 10^{-16} \text{ cm}^2$ (the Mn^{2+} ion has the same charge as the Zn^{2+} ion). The other typical values are: $E_{\text{em}} = 2 \text{ eV}$, $N = 10^{20} \text{ cm}^{-3}$, and $F = 10^6 \text{ V cm}^{-1}$. It follows that the energy efficiency equals about 2 %, which is in very good agreement with experiment. In this treatment, however, we have used a number of simplifications. We did not account for the Stokes shift. Moreover, we neglected light trapping effects in the thin layers. All these phenomena further reduce the energy efficiency. The energy efficiency is not likely to be improved significantly. This is mainly a consequence of the low value for the cross-section, because the value chosen for N cannot be too large in view of concentration quenching.

The mean energy the charge carrier has taken up from the electric field between two impact excitation events, neglecting any losses from phonon emission, equals $eF/\sigma N$. The minimum pathway L_{crit} that an electron has to travel to be able to excite an activator ion is $L_{\text{crit}} = E_{\text{exc}}/eF$, where E_{exc} is the energy needed for the excitation of the luminescence. Note

that L_{crit} is dependent on the electric field strength. Incorporation of L_{crit} in Equation (6) yields Equation (7). In case of the excitation of luminescence through host–lattice states, the luminescence efficiency can be written very generally as Equation (8).

$$\eta = E_{\text{em}}/E_{\text{exc}} * \sigma N * L_{\text{crit}} \quad (7)$$

$$\eta = E_{\text{em}}/E_{\text{exc}} * \eta_i * \eta_{\text{act}} * \eta_{\text{esc}} \quad (8)$$

In this expression η_i is the probability of energy transfer from the host lattice to the activator ions, η_{act} is the quantum efficiency of the activator, and finally η_{esc} is the escape probability, the ratio between the number of photons leaving the material and the number of photons generated in the material. By assuming η_{act} and η_{esc} to be unity, the maximum energy efficiency for the ACTFEL process is given by Equation (9).

$$\eta = E_{\text{em}}/E_{\text{exc}} * \eta_i \quad (9)$$

Inspection of Equations (7) and (9) leads to the conclusion that $N * L_{\text{crit}}$ is the transfer efficiency. In the case of cathode ray excitation, this figure can be unity, as it is for efficient cathode ray phosphors. In the case of ZnS:Mn its optimal value is calculated to be about only 0.02. The low transfer efficiency of energy from the host lattice states to activator states is the main reason for the low energy efficiency of this material but still it is the most efficient one known!

The number of efficient ACTFEL materials known is rather small. In particular, an efficient blue emitting material is lacking, which is the reason that full color displays are not yet on the market. Recently, SrS:Cu has been presented as an efficient blue electroluminescent phosphor,^[69] however, deposition as a thin film is a problem that has yet to be overcome. A general theory describing EL still needs to be developed, which is hampering a guided search for a blue emitter. The most important materials are summarized in Table 9. The EBU efficacy is the efficacy obtained after appropriate filtering to ensure that the emission spectrum complies with EBU standards.

Table 9. Overview of the most efficient EL phosphors.

Phosphor	Efficacy [lm W ⁻¹]	EBU efficacy [lm W ⁻¹]	Color
ZnS:Mn	5.0	1.1	red
ZnS:Tb	0.8	0.8 (no filter required)	green
SrS:Ce	1.6 ^[66]	0.07	blue
CaGa ₂ S ₄ :Ce	0.1 ^[67]	0.025	blue

From the figures in the table we can calculate, using a procedure not outlined here, a screen efficacy (for white light) of 0.44 lm W⁻¹ for SrS:Ce as blue primary and 0.27 lm W⁻¹ for the thiogallate as blue primary for electroluminescence displays complying with EBU standards with the three colour structure. Using the same procedure an efficacy of about 3 lm W⁻¹ is calculated for CRTs (see Section 4.1).

In Table 10 efficacies are given for a white emitting SrS:Ce/ZnS:Mn multilayer after filtering to three primary colors, together with the resulting color coordinates. For green and

Table 10. Efficacy for the three primary colors obtained after filtering from a white emitting SrS:Ce/ZnS:Mn multilayer.

	Efficacy [lm W ⁻¹]	CIE x- coordinate	CIE y- coordinate
no filter	2.0 [68]	0.39	0.48
red	0.11	0.65	0.34
green	0.26	0.20	0.61
blue	0.06	0.13	0.26

blue, there are deviations from EBU (for green $0.28 < x < 0.315$ for $y = 0.61$, for blue $y < 0.072$ and $x > 0.143$). From these data, a screen efficacy of 0.18 lm W^{-1} is calculated for white light that results from additive mixing of the three primary colors. [68, 70, 71]

On judging the brightness figures for electroluminescence displays, however, one has to keep in mind that in electroluminescence displays contrast is higher than in CRTs with the same luminance as a result of the use of non-scattering thin films and color filters.

Electroluminescent Organic Materials

Activity in the field of organic EL increased dramatically in 1987 when C. W. Tang and co-workers presented an organic thin film device based on low molecular weight (LMW) materials. This device demonstrated for the first time that light can be generated efficiently by direct recombination of charge carriers in organic materials. [72] A typical organic LMW EL device structure is shown in Figure 15. A glass substrate is covered with a transparent conductor, in most cases indium tin oxide (ITO). In consecutive evaporation steps, a hole transport layer (HTL), optionally an emissive layer, an electron transport layer (ETL), and finally a cathode are stacked on each other. The chemical requirements on charge transport layers and the organic emitter are quite stringent. The materials have to be evaporable without decomposition, they must have a high glass transition temperature (T_g) to prevent crystallization at elevated temperatures, and they have to be extremely chemically stable. Hole transport materials are based on aromatic amines known for their low oxidation potential and high hole mobility. [73] In order to prevent crystallization the amine phenyl groups often carry sterically demanding substituents. A prominent representative that is extensively used as hole transport material in photocopy machines and laser printers is TPD (Figure 15). [72, 74] The most frequently used electron transport material is a complex of aluminum with 8-hydroxyquinoline (AlQ, Figure 15) because it has good mor-

phological stability. This is important because usually very thin films of AlQ are applied to overcome the low electron mobility of the material. A device with only AlQ and a HTL already displays electroluminescence, however only with low efficiency. Stable organic fluorescent dyes doped in small amounts into the ETL (or sandwiched between the ETL and HTL) greatly enhance the electroluminescence efficiency and the device stability. [75] Similar to an inorganic phosphor, radiative transitions that follow energy transfer from the host to the dopant (see below) can be very effective when concentration quenching is avoided. Also, the choice of the fluorescent dye allows color tuning of the EL emission. Typical dopants are quinacridone (green), coumarin 6 (green), or rubrene (orange). [76] Blue EL has been achieved by perylene dopants in combination with a modified ETL; [77] in this context spiro compounds might be an interesting option as well. [78] Metals with a low working function such as Li, Ca, Mg, or alloys of them with Al or Ag are typically used as cathodes. [79]

The principle of EL in organic materials is explained in Figure 15. [80] A DC voltage, usually about 5 to 10 V is applied to the EL device between the ITO and metal cathode layer.

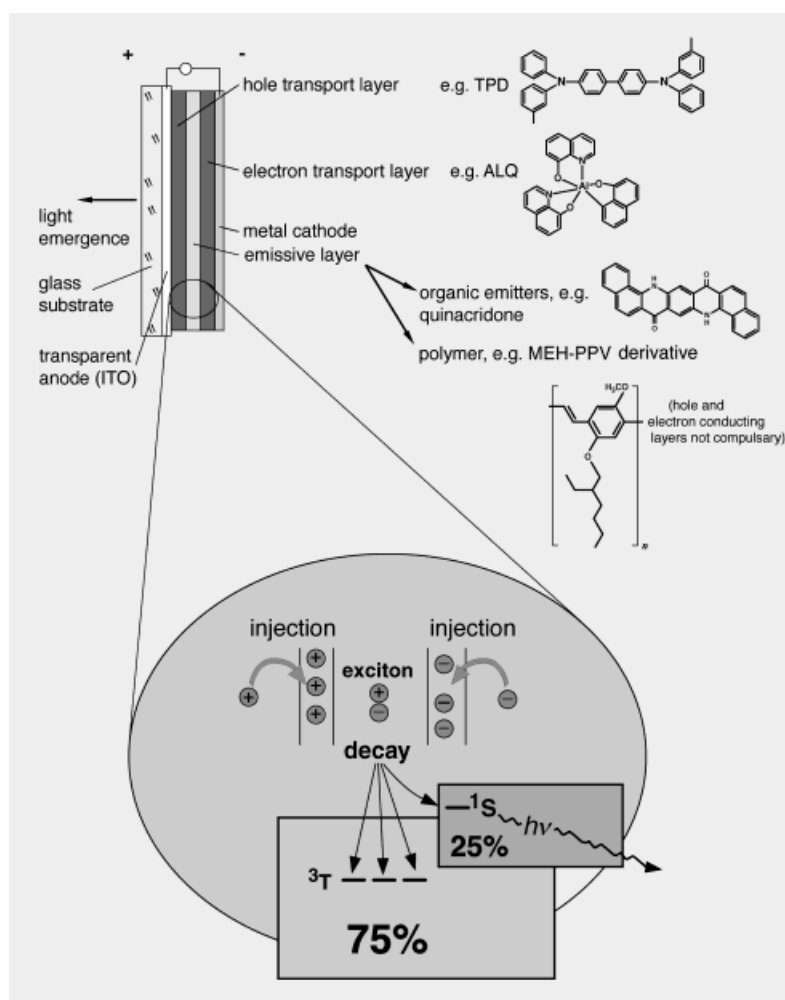


Figure 15. Top: Schematic diagram of an electroluminescent device showing the structural formulas of some commonly applied materials on the right. Bottom: Magnified illustration of the key processes of light generation in the device layers.

Positive charges are injected from the ITO into the HOMO of the HTL and electrons from the metal cathode into the LUMO of the ETL. For this step it is critical that the Fermi levels of the injecting layers and the accepting energy levels of the charge transport layers are adapted to each other in order to avoid injection barriers.^[81] At the same time, the build-up of space charge has to be avoided, which is possible by applying ultra-thin films of the charge transport layers in the order of few thousand angstroms or less.^[76] The HTLs are usually good electron blocking layers while the ETL can efficiently block positive charges. This means that the injected charges will be transported to the HTL–ETL interfacial region where the probability for recombination is maximized because of the potential barrier. Charge recombination leads to excitons, 25 % of which have singlet and 75 % triplet character on the basis of spin statistics.^[82] In organic fluorescent dyes only the ¹S state of the fluorescent dye can be populated, which in principle consequently decays radiatively with the same quantum yield as measured for photoluminescence. The triplet excitons are lost in nonradiative transitions or even photochemical side reactions that can be potentially harmful for the device stability. This drawback of organic fluorescent dyes has triggered efforts to use rare-earth ions, such as Eu³⁺ or Tb³⁺ coordinated to organic ligands, as emitters in organic EL materials.^[83] Here, the organic ligand acts as a sensitizer for the otherwise poorly absorbing rare-earth ion. In photoluminescence UV light is effectively absorbed by the organic ligand and leads to an excited singlet state. As a result of the close presence of the rare-earth metal ion intersystem crossing is effective in the compounds in which the ligand triplet state is populated. From there, the energy is efficiently transferred to the f levels of the lanthanide ion. In EL it appears likely that the ligand triplet levels can be populated directly after charge recombination. In theory, internal efficiencies of 100 % should thus be possible. Another advantage of rare-earth organic EL materials is the color purity of the generated emission (see Section 2), that is pure green and pure red for Eu- and Tb-activated devices, respectively.

From the above discussion on device structure it can be concluded that stability is a serious issue in organic EL materials. First, the cathode is highly corrosive, which means that oxygen and water have to be strictly avoided during device assembly. Alloy compounds can provide some degree of stabilization, but the device handling should still be performed in a dry box under argon. Second, the distance of the cathode to the anode is in the order of some 100 nm, which means an electrical field strength in the order of 10⁶ V cm⁻¹! Uneven substrates and impurities are a likely cause for short circuits. In industrial display development efforts concentrate on lowering the operation voltage and on sophisticated sealing techniques. A monochrome device basically consisting of TPD/AIQ doped with quinacridone has been realized with external efficiencies of up to 5 %^[84] and lifetimes of several thousand hours.

An alternative approach with a considerably simpler device structure is EL with polymer materials (PLEDs). Recently, certain polymers have been discovered that act at the same

time as charge transport and emissive layer.^[85] As shown in Figure 15, a typical PLED device consists of a polymer layer spin-coated or polymerized in-situ on a conducting substrate and an evaporated metal cathode. A variety of polymer materials has been synthesized spanning an EL color range from red to blue–green. The most prominent representative is poly(*p*-phenylenevinylene) PPV, and its derivatives, discovered by the group of R. H. Friend in 1990.^[86] A challenge of this material class is purity, which is not as readily achieved as with LMW materials where the evaporation step means a purification step at the same time. Also, the photoluminescence quantum yield, usually indicative of EL efficiency, of EL polymers is still inferior to low molecular weight materials. However, polymer EL has advanced impressively within only six years and flexible displays^[87] as well as polymer solid state lasers^[88] are within the scope of the polymer EL community.

5. Summary and Outlook

The clever tricolor concept, introduced in fluorescent lamps almost 30 years ago, together with the unique properties of rare-earth metal ions has revolutionized the lighting market. Both efficiency and light quality have been improved considerably. As a rather impressive result of about 50 years of phosphor research the luminescent materials applied in today's lamps and displays operate close to their physical limits, and improvements will most likely not be of a principal nature. New applications such as plasma display panels, inorganic electroluminescence, field emission displays, or mercury-free fluorescent lamps can fall back upon already developed materials; however, the introduction of new phosphors still appears likely. The direct conversion of electrical power into light by semiconductor LEDs and organic electroluminescence, the latter still in a very early stage, might reshape dramatically light generation in lighting and display applications. Primary plasma generation efficiencies and the downward energy cascade limit classical phosphor-based light generation to about 50 % maximum efficiency, while no principal limitations are foreseen for LEDs and organic electroluminescence. Although for these systems it is still a long way to go to compete with fluorescent lighting in price and efficiency, the already achieved performance with regard to lifetime and internal efficiency indicates clearly the future potential. Still indispensable for fine-tuning today's products and creating advanced products of tomorrow, classical phosphor development will likely give way to new, sophisticated forms of materials research. This work will be conducted increasingly under clean room conditions and many efforts will focus on thin film technologies. High-resolution full-color screens from laptop to home cinema size as well as much more efficient lighting sources than today's will be on the road ahead.

Abbreviations

ACTFEL	alternating current thin film electroluminescence
AIQ	aluminium-8-hydroxyquinolate

CIE	Commission Internationale d'Eclairage
CRI	color rendering index
CRT	cathode ray tube
CVD	chemical vapor deposition
EBU	European Broadcasting Union
EL	electroluminescence
ETL	electron transport layer
FED	field emission display
FWHM	full width at half maximum
HTL	hole transport layer
ITO	indium tin oxide
LCD	liquid crystal display
LCP	luminance contrast performance
LE	lumen equivalent
LED	light emitting diode
MOCVD	metal-organic chemical vapor deposition
PALC	plasma addressed liquid crystal
PCE	photon cascade emission
PDP	plasma display panel
PLED	polymer light emitting diodes
PPV	poly(<i>p</i> -phenylenevinylene)
PTV	projection television
QE	quantum efficiency
TPD	triphenyldiamine
TV	television
VUV	vacuum ultraviolet

Received: December 15, 1997

Revised version: May 22, 1998 [A 2641E]

German version: *Angew. Chem.* **1998**, *110*, 3250–3271

- [1] G. Blasse, *J. Alloys Compd.* **1995**, *225*, 529.
- [2] G. Blasse, B. C. Grabmeier, *Luminescent materials*, 1st ed., Springer, Berlin, **1994**.
- [3] a) K. A. Franz, W. G. Kehr, A. Siggel, J. Wiczorek, W. Adam in *Ullmanns Encyclopedia of Industrial Chemistry*, Vol A15, VCH, Weinheim, **1990**, p. 519; b) T. Welker, *J. Lumin.* **1991**, *48/49*, 49; c) G. Blasse, *J. Alloys Compd.* **1993**, *192*, 17; d) C. R. Ronda, *J. Alloys Compd.* **1995**, *225*, 534; e) C. R. Ronda, *J. Lumin.* **1997**, *72–74*, 49; f) C. R. Ronda, T. Jüstel, H. Nikol, *J. Alloys Compd.*, in press.
- [4] C. R. Ronda in *Spectroscopy and Dynamics of Collective Excitations in Solids*, Vol 356, Plenum, New York, **1997**, p. 339.
- [5] M. Bredol, U. Kynast, C. Ronda, *Adv. Mater.* **1991**, *3*, 361.
- [6] M. Bredol, U. Kynast, C. Ronda, *Chem. Unserer Zeit* **1994**, *28*, 36.
- [7] *Advances in Sonochemistry*, Vol 1–5 (Ed.: J. Mason), Jai Press, London, **1990–1998**.
- [8] B. Smets in *Advances in Nonradiative Processes and Solids*, Vol. 249 (Eds.: B. Di Bartolo, X. Chen), Plenum, New York, **1991**, p. 380.
- [9] K. H. Butler, *Fluorescent Lamp Phosphors*, The Pennsylvania State University Press, University Park, PA, **1980**.
- [10] W. J. van den Hoek, A. G. Jack in *Ullmanns Encyclopedia of Industrial Chemistry*, Vol A15, VCH, Weinheim, **1990**, p. 115.
- [11] C. Meyer, H. Nienhuis, *Discharge Lamps*, Kluwer, Deventer, **1988**.
- [12] L. Thorington, *J. Opt. Soc. Am.* **1950**, *40*, 579.
- [13] a) A. H. McKeag, P. W. Ranby (General Electric Company), GB-B 578.192, **1942**; b) H. G. Jenkins, A. H. McKeag, P. W. Ranby, *J. Electrochem. Soc.* **1949**, *96*, 1.
- [14] a) W. A. Thornton, *J. Opt. Soc. Am.* **1971**, *61*, 1155; b) M. Koedam, J. J. Opstelten, *Light. Res. Technol.* **1971**, *3*, 205; c) J. M. P. J. Versteegen, D. Radielovic, L. E. Vrenken, *J. Electrochem. Soc.* **1974**, *121*, 1627.
- [15] a) D. van der Voort, G. Blasse, *Chem. Mater.* **1991**, *3*, 1041; b) A. Bril, W. L. Wanmaker, *J. Electrochem. Soc.* **1964**, *111*, 1363; c) G. Blasse, A. Bril, W. C. Nieuwpoort, *J. Phys. Chem. Solids* **1966**, *27*, 1587; d) G. Blasse, A. Bril, *Philips Res. Repts.* **1967**, *22*, 46.
- [16] a) W. M. P. van Kemenade, H. C. G. Verhaar, *J. Mater. Chem. Phys.* **1992**, *31*, 213; b) R. Chapoulie, S. Dubernet, M. Schvoerer, *J. Mater. Chem. Phys.* **1991**, *30*, 47.
- [17] F. Wen-Tian, C. Fouassier, P. Hagenmuller, *Mater. Res. Bull.* **1987**, *22*, 899.
- [18] R. Jagannathan, *J. Lumin.* **1996**, *68*, 211.
- [19] J. Alarcon, D. van der Voort, G. Blasse, *Mater. Res. Bull.* **1992**, *27*, 467.
- [20] X.-D. Sun, C. Gao, J. Wang, X.-D. Xiang, *Appl. Phys. Lett.* **1997**, *70*, 3353.
- [21] E. Danielson, J. H. Golden, E. W. McFarland, C. M. Reaves, W. H. Weinberg, X. D. Wu, *Nature* **1997**, *389*, 944.
- [22] a) T. Arakawa, T. Takata, G.-Y. Adachi, J. Shiokawa, *J. Lumin.* **1979**, *20*, 325; b) O. A. Serra, E. J. Nassar, G. Zapparoli, I. L. V. Rosa, *J. Alloys Compd.* **1995**, *225*, 63; c) S. B. Hong, J. S. Seo, C.-H. Pyun, C.-H. Kim, Y. S. Uh, *Catal. Lett.* **1995**, *30*, 87; d) G. Blasse, G. J. Dirksen, M. E. Brechley, M. T. Weller, *Chem. Phys. Lett.* **1995**, *234*, 177.
- [23] a) C. Borgmann, J. Sauer, T. Jüstel, F. Schüth, U. Kynast, unpublished results; b) C. Borgmann, T. Jüstel, F. Schüth (Philips N.V.), EP-B 972016653, **1997**.
- [24] F. J. Avella, O. J. Sovers, C. S. Wiggins, *J. Electrochem. Soc.* **1967**, *114*, 613.
- [25] T. Jüstel, C. Ronda (Philips N.V.), EP-B 96202416.2, **1996**.
- [26] G. Blasse, M. Saakes, M. Leskela, *Mater. Res. Bull.* **1984**, *19*, 83.
- [27] M. V. Hoffmann, *J. Illum. Eng. Soc.* **1977**, *17*, 89.
- [28] a) M. Ouwerkerk, D. M. de Leeuw, C. A. Mutsaers, G. P. J. Geelen (Philips N.V.), EP-B 0550937 A2, **1993**; b) G. H. van der Linden, A. J. de Ridder, B. M. Smets (Philips N.V.) EP-B 0552513 A1, **1993**.
- [29] E. C. Malarkey, M. R. Natale, J. W. Ogland (Westinghouse Electric Corporation), US-A 3,766,084, **1973**.
- [30] R. Doeckel, F. A. S. Ligthart (Philips N.V.), DE-B 3544800 A1, **1987**.
- [31] A. R. Young, *Eur. J. Dermatol.* **1996**, *6*, 225.
- [32] L. Endres (Patent-Treuhand-Gesellschaft für elektrische Glühlampen mbH), DE-B 3729711 A1, **1989**.
- [33] P. J. M. Willemsen, R. C. Peters, W. L. Konijndijk (Philips N.V.), DE-B 3024438 A1, **1981**.
- [34] D. E. Harrison, *J. Electrochem. Soc.* **1960**, *107*, 210.
- [35] S. Sakka, *Struct. Bonding (Berlin)* **1996**, *85*, 3.
- [36] W. S. Rees, *CVD of Nonmetals*, Wiley-VCH, Weinheim, **1996**.
- [37] C. R. Ronda, *Proc. 2nd Int. Display Workshops* (Hamamatsu, Japan) **1995**, 69.
- [38] F. Vollkommer, L. Hitzschke (Patent-Treuhand-Gesellschaft für elektrische Glühlampen mbH), WO-A 94/23442, **1994**.
- [39] a) W. W. Piper, J. A. DeLuca, F. S. Ham, *J. Lumin.* **1974**, *8*, 344; b) J. L. Sommerdijk, A. Bril, A. W. de Jager, *J. Lumin.* **1974**, *8*, 341.
- [40] A. M. Srivastava, W. W. Beers, *J. Lumin.* **1997**, *71*, 285.
- [41] A. M. Srivastava, D. A. Doughty, W. W. Beers, *J. Electrochem. Soc.* **1997**, *144*, L190.
- [42] A. M. Srivastava, D. A. Doughty, W. W. Beers, *J. Electrochem. Soc.* **1996**, *143*, 4113.
- [43] R. T. Wegh, H. Donker, A. Meijerink, *Abstr. Pap. 192. Meeting of the Electrochemical Society (Paris)* **1997**, p. 1766.
- [44] a) S. Nakamura, G. Fasol, *The Blue Laser Diode*, Springer, Berlin, **1997**; b) S. Nakamura, *MRS Bulletin* **1997**, 29.
- [45] a) A. Dodabalapur, *Solid State Commun.* **1997**, *102*, 259; b) W. Gebhardt, B. Hahn, H. Stanzl, M. Deufel, *J. Cryst. Growth* **1996**, *159*, 238; c) T. Matsuoka, *Adv. Mater.* **1996**, *8*, 469; d) S. Strite, in *Advances in Solid State, Festkörperprobleme Series* (Ed.: H.-J. Queisser), Springer, Berlin, **1994**.
- [46] Regularly updated news on GaN based LEDs and lasers can be found in the online *MRS Internet Journal of Nitride Semiconductor Research* under <http://nsr.mij.mrs.org/>.
- [47] P. Schlotter, R. Schmidt, J. Schneider, *Appl. Phys.* **1997**, *A64*, 417.
- [48] F. Hide, P. Kozodoy, S. P. Denbaars, A. J. Heeger, *Appl. Phys. Lett.* **1997**, *70*, 2664.
- [49] V. Balzani, F. Scandola, *Supramolecular Chemistry*, Ellis Horwood, New York, **1991**.
- [50] Y. Sato, N. Takahashi, S. Sato, *Jpn. J. Appl. Phys.* **1996**, *35*, L838.
- [51] H. Boerner, T. Jüstel, H. Nikol, C. Ronda (Philips N.V.) DE-B 19708407.9, **1997**.
- [52] T. Hase, T. Kano, E. Nakazawa, H. Yamamoto, *Adv. Electron. Electron Phys.* **1990**, *79*, 271.

- [53] a) S. Shionoya in *Luminescence of Inorganic Solids* (Ed.: P. Goldberg), Academic Press, London, **1966**, p. 205; b) K. Era, S. Shionoya, Y. Washizawa, *J. Phys. Chem. Solids* **1968**, 29, 1827; c) K. Era, S. Shionoya, Y. Washizawa, H. Ohmatsu, *J. Phys. Chem. Solids* **1968**, 29, 1843.
- [54] H. Yamamoto, H. Matsukiyo, *J. Lumin.* **1991**, 48/49, 43.
- [55] a) C. R. Ronda, H. Bechtel, U. Kynast, T. Welker, *J. Appl. Phys.* **1994**, 75, 4631; b) T. Welker, C. R. Ronda, K. J. B. M. Nieuwesteeg, *J. Electrochem. Soc.* **1991**, 138, 602; c) C. R. Ronda, H. Bechtel, U. Kynast, T. Welker, *Eur. J. Solid State Inorg. Chem.* **1991**, 28 (suppl.), 545.
- [56] P. C. Candry, *Proc. 15th Int. Display Res. Conf.* (Hamamatsu, Japan) **1995**, 75.
- [57] a) M. Schadt, *Ann. R. Mater.* **1997**, 27, 305; b) H. Katoh, *Proc. 15th Int. Display Res. Conf.* (Hamamatsu, Japan) **1995**, 689; c) for updated information see *Stanford Resources, Inc.* under <http://www.webcom.com/sr/main/homepage.html>.
- [58] H. Bechtel, W. Czarnojan, M. Haase, W. Mayr, H. Nikol, *Philips J. Res.* **1996**, 50, 433.
- [59] S. Itoh, T. Kimizuka, T. Tonegawa, *J. Electrochem. Soc.* **1989**, 136, 1819.
- [60] S. Itoh, T. Wanatabe, T. Yamaura, K. Yano, *Proc. 15th Int. Display Res. Conf.* (Hamamatsu, Japan) **1995**, 617.
- [61] B. E. Gnade, *Abstr. Pap. 3rd Int. Conf. Sci. Technol. Display Phosphors* (Huntington Beach) **1997**, 1.
- [62] E. Yamaguchi, K. Sakai, I. Nomura, T. Ono, M. Yamanobe, N. Abe, T. Hara, K. Hatanaka, Y. Osada, H. Yamamoto, T. Nakagiri, *J. SID* **1997**, 5/4, 345.
- [63] L. F. Weber, *Proc. 15th Int. Display Res. Conf.* (Hamamatsu, Japan) **1995**, 373.
- [64] J. Koike, *Abstr. Pap. 3rd Int. Conf. Sci. Technol. Display Phosphors* (Huntington Beach) **1997**, 13.
- [65] C. R. Ronda, T. Amrein, *J. Lumin.* **1996**, 69, 245.
- [66] C. Barthou, J. Benoit, P. Benalloul, A. Morell, *J. Electrochem. Soc.* **1994**, 141, 524.
- [67] a) Y. A. Ono, *Electroluminescent Displays*, World Scientific, Singapore, **1995**; b) A. Pakkala, *ITG-Fachbericht Display and Vacuum Electronics*, VDE, Berlin, **1998**, p. 85.
- [68] a) R. H. Mauch, K. O. Velthaus, B. Hüttel, U. Troppenz, R. Herrmann, *SID'95 Int. Symp. Digest Technical Papers* (Orlando) **1995**, 720. b) K.-O. Velthaus, *ITG-Fachbericht Display and Vacuum Electronics*, VDE, Berlin, **1998**, p. 93.
- [69] W. Park, T. C. Jones, W. Tong, B. K. Wagner, C. J. Summers, *Abstr. Pap. 3rd Int. Conf. Sci. Technol. Display Phosphors* (Huntington Beach) **1997**, 57.
- [70] W. A. Barrow, R. C. Coovet, E. Dickey, C. N. King, C. Laakso, S. S. Sun, R. T. Tüenge, R. Wentross, J. Kane, *SID'93, Digest of Technical Papers* (Seattle) **1993**, 761.
- [71] K. O. Velthaus, B. Hüttel, U. Troppenz, R. Herrmann, R. H. Mauch, *SID'97 Int. Symp. Digest Technical Papers* (Boston) **1997**, 411.
- [72] C. W. Tang, S. A. Van Slyke, *Appl. Phys. Lett.* **1987**, 51, 913.
- [73] P. M. Borsenberger, J. J. Fitzgerald, *J. Phys. Chem.* **1993**, 97, 4815.
- [74] C. Adachi, S. Tokito, T. Tsutsui, S. Saito, *Jpn. J. Appl. Phys.* **1988**, 27, L269.
- [75] C. W. Tang, S. A. Van Slyke, C. H. Chen, *J. Appl. Phys.* **1989**, 65, 3610.
- [76] C. W. Tang, *J. SID* **1997**, 5/1, 11.
- [77] S. A. Van Slyke, P. S. Bryan, C. W. Tang in *Inorganic and organic electroluminescence/ EL 96 Berlin* (Eds.: R. H. Mauch, H.-E. Gumlich), W&T, Berlin, **1996**, p. 195.
- [78] J. Salbeck in *Inorganic and organic electroluminescence/ EL 96 Berlin* (Eds.: R. H. Mauch, H.-E. Gumlich), W&T, Berlin, **1996**, p. 243.
- [79] a) S. Saito, T. Tsutsui, M. Era, *Mol. Cryst. Liq. Cryst. Sci. Technol. Sect. A* **1994**, 253, 417; b) T. Wakimoto, S. Kawami, K. Nayama, *Tech. Dig. Int. Symp. Inorg. Org. Electrolumin.* **1994**, 77.
- [80] J. Schöbel, A. Böhrer, S. Dirr, H.-H. Johannes, A. Rückmann, P. Urbach, S. Wiese, W. Kowalsky, *ITG-Fachbericht Display and Vacuum Electronics*, VDE, Berlin, **1998**, 99.
- [81] M. Deußen, H. Bässler, *Chem. Unserer Zeit* **1997**, 31, 76.
- [82] M. Pope, C. E. Swenberg, *Electronic Processes in Organic Crystals*, Clarendon, Oxford, **1982**.
- [83] a) J. Kido, W. Ikeda, M. Kimura, K. Nai, *Jpn. J. Appl. Phys.* **1996**, 35, L394; b) J. Kido, H. Hayase, K. Hongawa, K. Nai, K. Okuyama, *Appl. Phys. Lett.* **1994**, 65, 2124; c) J. Kido, K. Nai, Y. Okamoto, T. Skotheim, *Chem. Lett.* **1991**, 1267; d) J. Kido, K. Nagai, Y. Ohashi, *Chem. Lett.* **1990**, 657; e) H. Boerner, U. Kynast, W. Busselt, M. Haase (Philips N.V.) DE-B P4428450.0, **1994**; f) H. Boerner, W. Busselt, T. Jüstel, H. Nikol (Philips N.V.), DE-B 19726472.7, **1997**.
- [84] Organic EL external quantum efficiency η is defined as $\eta = \eta(\text{charge recombination}) \times \eta(\text{energy transfer}) \times \Phi(\text{phosphor}) \times \eta(\text{light outcoupling})$; maximal values (approximation) are: 0.25 (only singlet exciton energy transfer) $\times 1 \times 1 \times 0.2$ (light guiding within the glass substrate).
- [85] a) A. Kraft, A. C. Grimsdale, A. B. Holmes, *Angew. Chem.* **1998**, 110, 416; *Angew. Chem. Int. Ed.* **1998**, 37, 402; b) N. Yu, H. Schenk, H. Spreitzer, W. Kreuder, H. Becker, *ITG-Fachbericht Display and Vacuum Electronics*, VDE-Verlag GMBH, Berlin, **1998**, 79.
- [86] J. H. Burroughes, D. D. C. Bradley, A. R. Brown, R. N. Marks, K. Mackay, R. H. Friend, P. L. Burn, A. B. Holmes, *Nature* **1990**, 347, 539.
- [87] See for example: D. Braun, A. R. Brown, E. Staring, E. W. Meijer, *Synth. Met.* **1994**, 65, 85.
- [88] N. Tessler, G. J. Denton, R. H. Friend, *Nature* **1996**, 382, 695.